ABSTRACT

WORTHINGTON, CAROLYN JEAN. Evidence for Recombination, Heterosis and Toxigenesis in Experimental Hybrid Crosses Between *Aspergillus flavus* and *Aspergillus parasiticus.* (Under the direction of Dr. Ignazio Carbone.)

Aspergillus flavus and *A. parasiticus* are two of the most important aflatoxin-producing species that contaminate agricultural commodities worldwide. Both species are heterothallic and have been shown to undergo sexual reproduction in laboratory crosses. In this thesis I examined the possibility of interspecific matings between *A. flavus* and *A. parasiticus*. These species can be distinguished morphologically and genetically, as well as functionally via the biosynthesis of specific aflatoxins and an unrelated mycotoxin, cyclopiazonic acid (CPA). *Aspergillus flavus* produces B aflatoxins and CPA, B aflatoxins or CPA alone, or neither mycotoxin; *A. parasiticus* produces B and G aflatoxins or *O*-methylsterigmatocystin (OMST) but not CPA. Only four out of forty-five attempted interspecific crosses between compatible mating types of *A. flavus* and *A. parasiticus* were fertile. Single ascospore strains from each cross were isolated and shown to be hybrids using array comparative genome hybridization (aCGH) and multilocus sequence typing (MLST). Higher mean concentrations of B_1, B_2, G_1 and G_2 aflatoxins in addition to CPA in the F1 progeny compared to midpoint parent toxin levels indicate high heritability across the aflatoxin and CPA clusters as well as heterosis in both. Three progeny synthesized G_1 and G_2 aflatoxins that were not produced by the parents, which indicate that hybridization may be important in the genesis of unique hybrid toxin profiles. The tight clustering of experimental hybrids with naturally occurring *A. flavus* S strains and *A. nomius* based on aCGH and MLST suggests that hybridization may be driving genetic and functional diversity and the emergence of super-toxin producing strains.

Evidence for Recombination, Heterosis and Toxigenesis in Experimental Hybrid Crosses Between *Aspergillus flavus* and *Aspergillus parasiticus*

by
Carolyn Jean Worthington

A thesis submitted to the Graduate Faculty of
North Carolina State University
in partial fulfillment of the
requirements for the degree of
Master of Science

Plant Pathology

Raleigh, North Carolina

2011

APPROVED BY:

_____	_____
Dr. Gary A. Payne	Dr. Peter Ojiambo

_____
Dr. Ignazio Carbone
Chair of Advisory Committee

DEDICATION

To God, through Whom all things are possible.

To my husband, Frank, for being tremendous support and encouragement.

In remembrance of my late father, Earl Daugherty.

BIOGRAPHY

Carolyn Jean Worthington obtained her BS in Biological Sciences from North Carolina State University in 2008, where she began working in Dr. Ignazio Carbone's lab as an undergraduate technician studying mating type idiomorphs in *Aspergillus* section *Flavi* and mitochondrial inheritance in *Petromyces parasiticus*. She is interested in determining the mechanisms of heterosis through analyzing interspecific crosses between *Aspergillus flavus* and *A. parasiticus* for mycotoxin diversity and genome heterogeneity. A long-term goal is to provide a better understanding of natural population structure and adaptation according to environmental and host conditions.

ACKNOWLEDGMENTS

I would like to thank my advisory committee—Dr. Gary A. Payne and Dr. Peter Ojiambo—for their time and advice; and especially my major advisor, Dr. Ignazio Carbone, for his expert guidance through this process. I am grateful to the co-contributors without whom this work would not have been possible: Dr. Bruce Horn for his painstaking work isolating the original soil isolates, setting up and babysitting the crosses, and for providing the toxin assays; Dr. Geromy Moore for his contribution of the beautiful SEM and LM work, and for his work in genotyping the natural isolates; J. Trent Monacell for the generation and analysis of the images from aCGH; Dr. Eric Stone for his expertise with statistical analysis; and Rakhi Singh for her help with preparing the DNA for aCGH and lab support in general. I would also like to thank all the past and present members of the Carbone Mafia for their support. I also thank Milbra Schweikert for her technical expertise with the toxin assays; and Valerie Knowlton for her assistance with the Scanning Electron Microscopy.

TABLE OF CONTENTS

LIST OF TABLES vi
LIST OF FIGURES vii
Chapter 1 1
GENERAL INTRODUCTION 1
Pathogen Characteristics and Life Cycle 1
Crop Loss and Biocontrols 2
Hybridization and Heterosis Occurrences 3
Summary 5
Chapter 2 6
INTRODUCTION 6
MATERIALS AND METHODS 8
Interspecific Crosses 8
Light Microscopy and SEM 9
Mycotoxin Quantification and Heritability 10
DNA Extraction and Multilocus Sequencing 11
MLSTs 11
Array Comparative Genome Hybridization (aCGH) 12
Heat Maps and Genome-Wide Dendrogram 14
Parent-Offspring Trio Heat Maps 15
Genome-Wide Parentage Plots 16
Principle Component and Phylogenetic Analysis 17
RESULTS 18
Interspecific Crosses 18
Light Microscopy and SEM 18
Mycotoxin Quantification and Heritability 19
MLSTs 19
Heat Maps and Genome-Wide Dendrogram 20
Parent-Offspring Trio Heat Maps 21
Genome-Wide Parentage Plots 21
Principle Component and Phylogenetic 23
DISCUSSION 23
REFERENCES 29

LIST OF TABLES

Table 1 Incidences of sexual state in forty-five attempted interspecific crosses between compatible mating types of *Aspergillus flavus* and *A. parasiticus*. 36

Table 2 Multilocus genotypes and mycotoxin phenotypes from four most fertile interspecific crosses between *Aspergillus flavus* and *A. parasiticus* 44

Table 3 Predicted genes on the right arm of chromosome 3 of *Aspergillus flavus* 47

LIST OF FIGURES

Figure 1 Chemical structures of OMST, B and G aflatoxins, and CPA 51

Figure 2 Sexual reproductive structures observed in hybrid crosses between *Aspergillus flavus* and *A. parasiticus* 52

Figure 3 Aflatoxin and CPA heritability in intra and interspecific crosses of *A. flavus* and *A. parasiticus*. 54

Figure 4 Genome-wide similarity dendrogram based on aCGH data of a representative sample of fifty-six isolates representing variation in intra and interspecific crosses, natural isolates sampled from populations of *A. flavus* and *A. parasiticus* and closely related species in *Aspergillus* section *Flavi* 55

Figure 5 Heat maps showing aCGH patterns in the CPA, aflatoxin and sugar clusters in the right arm of chromosome 3; the strains are ordered based on clades inferred from genome-wide aCGH analysis in Figure 4. 57

Figure 6 Heat maps of six *Aspergillus flavus* and *A. parasiticus* parent-offspring trios for the chromosomal region shown in Figure 5 59

Figure 7 Genome-wide parentage plots **(A-F)** for the six parent-offspring trio heat maps shown in Figure 6 61

Figure 8 Maximum likelihood phylogenetic and principle component analyses based on MLSTs (*aflM, aflW* and *trpC*) showing clustering and association with quantitative variation in aflatoxin production between experimental hybrid strains and natural isolates of *A. parasiticus*, *A. flavus* L, S_{BG} and S_B sampled from populations on a global scale **(A)** and within the US alone **(B)**. 67

CHAPTER 1

GENERAL INTRODUCTION

Pathogen Characteristics and Life Cycle Members of *Aspergillus* section *Flavi*, in the fungal phyllum Ascomycota, are opportunistic pathogens and saprophytes of crops such as corn, cotton, peanuts, soybeans and other tree nuts; as well as opportunistic human and animal pathogens. Among section *Flavi*, *Aspergillus flavus* is most notable for giving its namesake to the potent mycotoxin, aflatoxin, However, there are other non-toxin-producing members in the group (Klich 2007). In agricultural commodities, *Aspergillus flavus* is most commonly found on corn and peanuts in the Southern United States, and cotton and tree nuts in the Western United States (Payne 1998). *Aspergillus parasiticus* is often found in the soil along with *A. flavus*, and poses no less risk to host crops.

The primary inoculum is the anamorphic, or asexual, spore called a conidium. Conidia are thought to travel short distances aerially on wind currents above the canopy level of crops, or can be transported by insects. Once conidia have germinated on host tissue, crop loss can occur before or after harvest, from tissue degeneration due to fungal invasion or from contamination by mycotoxins. *Aspergillus fumigatus* has long been known as a human pathogen, but the number of reports of human infection from *Aspergillus flavus* is growing. If conidia are inhaled by immunocompromised humans, they can germinate in the lung tissue causing blockage and a condition called aspergillosis (Hedayati *et al.* 2007). The growing tissues of the fungus--hyphae-- form a mass of mycelium in the culture and can then produce either conidia or sclerotia, or both.

Sclerotia, the asexual over-wintering structures, can persist in the soil or crop debris and germinate once conditions are again favorable. *Aspergillus*, as opposed to most fungi, prefers hot dry conditions and is also thought to produce higher levels of dangerous toxins in these conditions also (Horn & Greene 1995).

Until 2009, *Aspergillus flavus* and *A. parasiticus* were thought to only have a vegetative state. Variation among species was classified into vegetative compatibility groups (VCGs) or heterokaryon compatibility (h-c) groups (Papa 1986). Although currently classified as two distinct species, *Aspergillus flavus* and *A. parasiticus* share similarity in their sexual, or teleomorphic, structures (Horn *et al.* 2009a; Horn *et al.* 2009c). Both species house their sexual spores (ascospores) in asci located within an ascocarp. The ascocarp is formed inside a structure very similar to a sclerotium, termed a stroma if sexual structures are present. Although *Aspergillus flavus* and *A. parasiticus* are referred to as *Petromyces flavus* and *P. parasiticus*, respectively, in the teleomorphic state (Horn *et al.* 2009a; Horn *et al.* 2009c), these terms have not been widely accepted. Prior to 2009, the sexual structures of *A. flavus* and *A. parasiticus* had not been discovered; although, the mating type genes, sexual structures and sexual cycle in other filamentous ascomycetes had been previously described (Coppin *et al.* 1997). Also prior to the discovery of sexual structures, Geiser and colleagues speculated the existence of sexual recombination based on distinct phylogenetic clades of *A. flavus* (Geiser *et al.* 1998).

Crop Loss and Biocontrol Contamination of crops from *Aspergillus flavus* and *A. parasiticus* has been a severe problem in the United States (Horn & Dorner 1999) as well as

many other parts of the world including Kenya (Gieseker *et al.* 2004; Probst *et al.* 2007_ENREF_50), Thailand (Ehrlich *et al.* 2007) and Hungary (Fazekas *et al.* 2005); and contributes to lost food sources for both humans and animals. It is estimated that mycotoxin contamination, causes in excess of $1.66 billion dollars in total loss each year (Vardon *et al.* 2003). In 2001, it was estimated that aflatoxin cost the peanut industry alone over $25 million annually (Lamb & Sternitzke 2001). To date, there is no known resistance to *Aspergillus* infection on crops. However, two biocontrol strains of *Aspergillus flavus* have been approved for application in agricultural fields. AF36 is a naturally occurring isolate from Arizona (Bigelow *et al.* 2001), which has a deletion in the *aflC* region of the aflatoxin gene cluster, rendering it atoxigenic (Moore *et al.* 2009). Afla-Guard® has been approved for the use on peanuts (Dorner 2005), and is missing the entire aflatoxin gene cluster, also rendering it atoxigenic (Moore *et al.* 2009). The purposed function of these strains is to outcompete indigenous potentially toxigenic strains, preventing toxin production.

Hybridization and Heterosis Occurrences In the discipline of mycology, the debate over speciation and taxonomy has been raging for quite some time. Because fungi are known to have varying life cycles, sometimes dependent upon the host organism or environment, it has been challenging to define sharp species boundaries. Studies of interspecific hybridization have been occurring for decades now, but the advent of molecular and evolutionary biology has made it possible to see the details and mechanisms at work (Schwenk *et al.* 2008). Andrew Hendry points out that hybrid speciation, the creation of new evolutionary clades through the fusion of two ancestral species, may be more widespread across kingdoms than

previously thought (Hendry 2009). It has also been suggested that hybrid speciation is a means of creating diversity in a population, or an entirely new species altogether (Mallet 2007). Further, the creation of new evolutionary paths or clades via selection based on fertility and viability in the processes of hybrid speciation could be a means to overcome genetic isolation and drift (Gross & Riesberg 2005). Although the motives behind hybridization are not yet clear, there are many possible benefits to interspecific recombination, including increasing genetic variation, overcoming environmental conditions, escaping genetic isolation, adapting to new host organisms, producing more or different secretory products and utilizing novel food sources. One example of hybridization providing better host adaptation comes from a study on plant associations with fungi and oomycetes. Of particular interest, and relevant to the current study, is the potential for heterosis, or "superpathogen" generation, through interspecific hybridization which may give rise to new host interactions (Schardl & Craven 2003) and increase the effective pathogen potential. In the case of *Aspergillus* section *Flavi*, this may mean the potential for greater mycotoxin production or possibly even novel toxin production. Another possible outcome of hybridization is the potential for an increased rate of evolution and also pathogenicity when two or more genomes are combined (Brasier 2000). This was seen in a hybrid *Phytophthora,* which was found to infect European alder as previously unreported. If *Aspergillus* has the same hybridization potential, this could mean survival outside of typical environmental conditions, or toxin production on atypical host crops.

Summary *Aspergillus flavus* and *A. parasiticus*, each by themselves, pose a threat to both crops and humans, depending on favorable environmental conditions. The damage caused by each is potentially detrimental to both crop loss and disease caused by mycotoxin contamination. However, with the possibility of hybridization and heterosis, the potential of the resulting progeny individuals could be better adapted to hostile environments or atypical host species. Another potential outcome is more aggressive pathogenicity on known hosts. The potential of these pathogens to create variability through recombination and hybridization, followed by maintaining these putative novel phenotypes through vegetative propagation creates a high-risk pathogen.

In addition to the agricultural and ecological impacts of hybridization, progeny hybrids between *Aspergillus flavus* and *A. parasiticus* could give us a better way to understand inheritance mechanisms. Although *A. flavus* and *A. parasiticus* are similar enough in structure and function to undergo sexual mating, they are still divergent enough to see single nucleotide polymorphisms (SNPs) between two parents of the different species (Godet & Munaut 2009). This phenomenon will give us the opportunity to observe inheritance mechanisms that may not otherwise have resolution in intraspecific crosses.

Also, a collection of hybrid progeny, complete with genotypic and phenotypic characteristics would be an invaluable resource to the mycological community. These progeny could be used to better understand mycotoxin control and inheritance in general.

CHAPTER 2

INTRODUCTION

Aflatoxins are a family of carcinogenic secondary metabolites commonly produced by species in *Aspergillus* section *Flavi*. *Aspergillus flavus* and *A. parasiticus* are the most extensively studied species because of their agricultural and medical importance. Both species have affinities for oilseeds but differ in the types of aflatoxins produced. While both *A. flavus* and *A. parasiticus* produce the B aflatoxins (B_1 and B_2), *A. parasiticus* also produces the G aflatoxins (G_1 and G_2). In addition to aflatoxins, *A. flavus* produces another unrelated mycotoxin, cyclopiazonic acid (CPA) that is highly detrimental to human and animal health (Burdock & Flamm 2000). Because of their high carcinogenic properties, federally and internationally mandated laws require the destruction or decontamination of the crop when the aflatoxin content exceeds 15 μg/kg, resulting in huge yield losses worldwide (Pitt 2000); currently there is no regulation of CPA (Abbas *et al.* 2011).

Natural populations of *A. flavus* show a high level of variation in mycotoxin production, with individuals producing both aflatoxins and CPA, aflatoxins alone, CPA alone or neither mycotoxin (Horn & Dorner 1999; Horn *et al.* 1996). *Aspergillus parasiticus* produces B and G aflatoxins or the precursor O-methylsterigmatocystin (OMST) but not CPA. *Aspergillus flavus* is further characterized by two morphotypes: the typical L strain with large sclerotia >400 μm in diameter and the S strain with

abundant small sclerotia <400 μm (Cotty 1989). Although nontoxigenics isolates are fairly common in L strains (Chang *et al.* 2005; Horn & Dorner 1999) and can predominate in certain fields (Ehrlich 2008), they are rare in *A. flavus* S strain and *A. parasiticus* (Horn & Dorner 1999). L strains typically produce B aflatoxins and CPA, whereas the S strains may produce B only (S_B) or B+G (S_{BG}) in addition to CPA (Horn 2005). The S_{BG} producers include *A. minisclerotigenus* (Pildain *et al.* 2008), *A. nomius* (Ehrlich *et al.* 2007), and *A. parvislerotigenus* (Frisvad *et al.* 2005).

Several population genetic studies report that recombination and selection may be important forces driving strain and chemotype diversification in *A. flavus* (Geiser *et al.* 1998; Moore *et al.* 2009), *A. parasiticus* (Carbone *et al.* 2007a) and *A. nomius* (Peterson *et al.* 2001). This hypothesis is further strengthened by the recent discovery of a sexual state in *A. flavus* (Horn *et al.* 2009a), *A. parasiticus* (Horn *et al.* 2009b, c) and *A. nomius* (Horn *et al.* 2011), providing the first direct evidence that sexual recombination may be an important mechanism for generating diversity in aflatoxin production in these species. An early study using DNA-DNA hybridization to examine the extent of nuclear DNA complementarity between *A. flavus, A. parasiticus* and their closely related nonaflatoxigenic species *A. oryzae* and *A. sojae* found that all four species have high (69-100%) DNA complementarity and overall similar genome size (Olarte *et al.* 2011). These results prompted the authors to propose that the four species represent morphological and physiological varieties of a single species, which they designated as *A. flavus*; in this case *A. flavus* and *A. parasiticus* would be considered subspecies of *A. flavus.*

Given the close similarity between *A. flavus* and *A. parasiticus* we explored the possibility of interspecific matings by taking full advantage of our knowledge of the mating system and fertility data from intraspecific crosses of *A. parasiticus* (Horn *et al.* 2009b) and *A. flavus* (Horn *et al.* 2009a; Olarte *et al.* 2011). My objectives are 1) to set up experimental matings between *A. flavus* and *A. parasiticus* and characterize progeny from fertile crosses using multilocus DNA sequence-based markers, genome-wide hybridization to *A. flavus* microarrays and quantitative mycotoxin assays, 2) to determine heritability of B and G aflatoxins and CPA across inter and intraspecific crosses, and examine the possibility of heterosis as related to mycotoxin phenotype, and 3) to compare genotypes and toxin profiles of hybrid progeny strains to isolates sampled from natural populations on a global scale and locally in the US.

MATERIALS AND METHODS

Interspecific Crosses Strains of *Aspergillus flavus* and *A. parasiticus* were obtained from soil and peanut seeds in three peanut fields from Terrell County, Georgia, USA, and have been characterized according to morphology, vegetative compatibility, and aflatoxin production (Horn & Greene 1995; Horn *et al.* 1996). In previous research, we grouped these strains into haplotypes (alleles) based on sequence variation in 21 intergenic regions of the aflatoxin gene cluster (Carbone *et al.* 2007a) and also identified their mating-type genes *MAT1-1* and *MAT1-2* (Ramirez-Prado *et al.* 2008). Forty-five crosses of sexually compatible *A. flavus* and *A. parasiticus* strains were set up

to examine the possibility of hybridization between the two species (see Table 1). Fungal strains were initially grown on Czapek agar (Cz) (Raper & Fennell 1965) slants for 14 days at 30 °C. Dry conidia from these cultures were paired strains of the opposite mating type in 0.2% (w/v) water agar containing 50 μL/L Tween 20 (approximately 5×10^5 conidia/mL of each strain). Conidial suspensions (7 μL) were spread onto each of five slants of mixed cereal agar (McAlpin & Wicklow 2005) (7 mL medium in 20 × 125-mm screw-cap test tubes), and slants were incubated in darkness for 14 days at 30 °C to induce sclerotium production. Slant cultures (caps loose) were then enclosed in sealed plastic bags to prevent desiccation and incubated an additional 6–9 months at 30 °C. For each interspecific cross, up to 300 sclerotia, when available, were sliced open and examined for ascocarps and ascospores. Single ascospore progeny isolates were obtained from individual ascocarps within stromata according to Horn et al. (2009).

Light Microscopy and SEM Stromata from two fertile *A. flavus x A. parasiticus* crosses (IC278 × IC324 and IC278 × IC327) that were among the crosses with the highest number of ascospore-bearing ascocarps (Table 1), were dissected and imaged using both light microscopy and scanning electron microscopy (SEM). Hand-sectioned stromata were examined using both a stereomicroscope and compound microscope. For SEM imaging, samples were fixed using a gluteraldehyde/sodium cacodylate buffer and critical-point dried, following the same protocol as in previous work (Horn *et al.* 2009b).

Mycotoxin Quantification and Heritability Vials (4 mL) of 1 mL of yeast-extract sucrose broth were inoculated with dry conidia (approximately 1 x 10^5) to determine AF and CPA production by parents and F1 hybrids (Horn & Dorner 1999). Cultures were maintained undisturbed in darkness for 7 days at 30°C. Production of AFs and CPA in vial cultures was analyzed by high performance liquid chromatography as previously described (Horn & Dorner 1999; Horn *et al.* 1996). Quantification limits are 0.5 ng of AF B_1 and 2 μg of CPA per mL of culture medium. Previously we determined that twelve offspring in each of four different *A. parasiticus* crosses (Horn *et al.* 2009b) were sufficient for precise estimates of AFs G_1, G_2, B_1, and B_2 heritability (Carbone, unpublished data). A similar experimental design was followed in the present study with eleven or twelve offspring examined for each of the four *A. flavus x A. parasiticus* crosses. Each individual progeny was sampled after seven days of growth and at three points within the culture slant—at the top, middle and bottom of the slant. These values were then averaged.

Average AF and CPA trait values of offspring were plotted against mid-parent values for each cross, and mycotoxin heritability was estimated as the slope of the resulting best-fit regression line. Heritabilities of $B_1 + B_2$, $G_1 + G_2$ and CPA in interspecific crosses were plotted with corresponding calculations in *A. flavus* and *A. parasiticus* intraspecific crosses (Figure 3). *O*-methylsterigmatocystin (OMST) was omitted from the heritability analysis since only the hybrid progeny were assayed for this mycotoxin precursor. To determine whether mycotoxin production in the hybrid

offspring of each interspecific cross was significantly higher than in the parental species we first tested for a significant difference in mean B_1, B_2, G_1, G_2 and CPA concentrations

between progeny and parental isolates using ANOVA followed by a comparison of means using Tukey's multiple comparisons test implemented in the R statistical software (R Development Core Team 2010). All tests were based on three biological replicates for each parental and progeny isolate.

DNA Extraction and Multilocus Sequencing Total genomic DNA was extracted from lyophilized mycelial pellets using either the Qiagen maxiprep kit (Qiagen, Valencia, CA) or the MasterPure Yeast DNA Purification Kit (Epicentre Technologies, Madison, WI). The pellets were first pulverized before extraction using a Retsch MM301 tissue homogenizer (Retsch, Inc., Newtown, PA). PCR amplifications and DNA sequencing for multilocus sequence typing (MLST) were based on sequences of oligonucleotide primers that were described previously (Moore *et al.* 2009, Carbone *et al.* 2007a). For each locus, DNA sequences were aligned and manually inspected using Sequencher Version 4.7 (Gene Codes Corporation, Ann Arbor, MI). Alignments were then exported as NEXUS files and imported into SNAP Workbench (Price & Carbone 2005). Alignments for each locus were clone-corrected by collapsing separately into unique haplotypes using SNAP Map (Aylor *et al.* 2006) and combining using SNAP Combine (Aylor *et al.* 2006) for inference of MLSTs. Haplotype collapsing was performed with the option of recoding insertions/deletions (indels) for maximal MLST resolution.

MLSTs Genome-wide recombination events arising from independent assortment of chromosomes were detected by examining MLSTs based on DNA sequence variation at four

loci that span three chromosomes: *aflM/aflN* and *aflW/aflX* located in the aflatoxin cluster on chromosome 3 and the mating type (*MAT*) and tryptophan synthase (*trpC*) genes located on chromosomes 6 and 4, respectively. For each locus, the null hypothesis of no significant difference in the frequency of parental alleles in the progeny sampled from each cross was tested using a binomial test implemented in MS Excel. In crosses that produce progeny with no crossovers in the AF cluster, we would expect Mendelian segregation of loci on different chromosomes to result in only $(0.5)^3$ or 13% of the progeny sharing a parental MLST. Within each cross, significant differences in toxin production between hybrid offspring and parental isolates were interpreted within the context of MLSTs based on four loci (*aflM*/*aflN*, *aflW*/*aflX*, *MAT*, and *trpC*) spanning three linkage groups. Specifically we examined whether progeny strains showed evidence of independent assortment, and whether progeny individuals that shared a multilocus haplotype had a significant difference in AF and CPA production.

We examined a cluster-specific MLST for reconstructing crossover events in the AF gene cluster. This was based on two intergenic regions in the AF cluster (*aflM/aflN* and *aflW/aflX*) that flank recombination hotspots in *A. flavus* (Moore *et al.* 2009) and *A. parasiticus* (Carbone *et al.* 2007a). A crossover between these loci in the parents would result in progeny genotypes with a different combination of parental alleles.

Array comparative genome hybridization (aCGH) Hybrid progeny showing unique mycotoxin phenotypes as well as independent assortment, as determined by MLSTs located on three separate chromosomes, were further subjected to aCGH along with their respective

parental strains to corroborate inferences from MLST-based genotyping and to possibly identify crossovers within the aflatoxin gene cluster. Fedorova and colleagues have shown that aCGH provides sufficient resolution to examine intraspecific genetic variation and strain-specific variation in gene content in *A. flavus* (Fedorova *et al.* 2009)—thus aCGH should also show significant interspecific resolution to distinguish between *A. flavus* and *A. parasiticus*. The aCGH of parent-offspring trios (two parents plus one progeny) were based on hybridization of total genomic DNA to whole genome *A. flavus* Affymetrix GeneChip microarrays, using the *A. flavus* genome strain, NRRL 3357. Each array comprises 12,834 predicted genes and 397 predicted antisense transcripts of NRRL 3357 (_ENREF_30Payne *et al.* 2008). Twelve 25-mer-oligonucleotide probes represent each gene and are located at the 3' end of the gene. The array was tiled, with partially overlapping probes in the intergenic regions of the AF biosynthetic pathway from *aflF* to *nadA,* to provide more coverage and increase resolution of putative crossovers. The BioPrime DNA labeling System (Invitrogen Catalogue No. 18094-011) was used to label genomic DNA as follows: (1) fungal DNA in the amount of 300-350 ng was mixed with 60 µl of 2.5X random primers (BioPrime kit) and 132 µl of dH_2O; (2) the reaction mixture was denatured in an Eppendorf thermocycler at 99 °C for 10 min and then cooled at 4 °C for 15 min; (3) 15 µl of 10X dNTPs containing biotin dCTP and 3 µl Klenow polymerase were added and incubated at 25 °C in a thermocycler for 18 h; (4) the reaction mixture was precipitated by adding 15 µl of 3M NaOAc and 400 µl of cold 95% ethanol, followed by incubation at 20 °C for 15 min; (5) samples were centrifuged at high speed in a refrigerated microcentrifuge for 20 min; and (6) the pellets were washed with 500 µl ice-cold 70% ethanol, centrifuged and then vacuum dried with heating for 10

min. DNA was resuspended in 100 μl of dH_2O, and 5 μl was used to check the quality of the labeled DNA using gel electrophoresis.

Hybridization and analysis of each sample was performed by Expression Analysis (Raleigh-Durham NC). Briefly, 300-350 ng of fragmented genomic DNA was diluted in hybridization buffer (MES, NaCl, EDTA, Tween 20, Herring Sperm DNA, Acetylated BSA) containing biotin-labeled OligoB2 and Eukaryotic Hybridization Controls (Affymetrix). The hybridization mixture was denatured at 99 °C for 5 minutes, incubated at 45 °C for 5 minutes and then injected into a GeneChip cartridge. The GeneChip array was incubated at 42 °C for at least 16 hours in a rotating oven at 60 rpm. GeneChips were washed with a series of nonstringent (25 °C) and stringent (50 °C) solutions containing variable amounts of MES, Tween20 and SSPE. The microarrays were then stained with streptavidin-phycoerythrin, and the fluorescent signal was amplified using a biotinylated antibody solution. Fluorescent images were detected in a GeneChip® Scanner 3000 and array data were extracted using the GeneChip Operating System v 1.1 (Affymetrix). The images were further inspected for quality and the absence of defects or debris. Quality control was based on a comparison of the conformity of hybridization controls, scaling factor, and noise; percent detection metrics were analyzed to determine if any outliers were present.

Heat Maps and Genome-Wide Dendrogram Array data for all strains examined using aCGH were imported into JMP genomics (SAS, Cary, NC, USA) for further transformation and normalization. All probe sets for genes between the telomere on the right arm of chromosome 3 (abbreviated 3R) up to the CPA cluster, for the adjacent AF cluster genes and

intergenic regions, and for the flanking sugar cluster genes were selected and ordered by their physical location on chromosome 3R (Table S1). Data were log2 transformed and normalized using Loess normalization. Since we are interested in detecting differences in hybridization intensities between the reference strain and our experimental isolates, no background correction was applied. The normalized and transformed data were exported in MS Excel format.

A similarity dendrogram based on aCGH data of a representative sample of fifty-six isolates representing variation in selected intra- and interspecific crosses, as well as natural isolates sampled from populations of *A. flavus* and *A. parasiticus* and closely related species in *Aspergillus* section *Flavi,* was generated in JMP genomics (Figure 4). A heat map and corresponding color scale for the telomeric/subtelomeric region of chromosome 3R was also automatically generated (Figure 5) using the imagesc function in Matlab (MathWorks Inc., Natick, MA).

Parent-Offspring Trio Heat Maps We evaluated parent/offspring transmission by comparing hybridization intensities for each of six parent-offspring trios (Figure 6). A simple squared difference between measurements was used and we aggregated the values within a window by summing across probes, as described previously (Olarte *et al.* 2011). In the analyses, p_j^1, p_j^2 and o_j denote the normalized probe j intensities for parent 1, parent 2 and their offspring, respectively. At polymorphic sites we expect the smaller of $\left(p_j^1 - o_j\right)^2$ and $\left(p_j^2 - o_j\right)^2$ to associate with inheritance and also expect a switch of parental origin at

recombination breakpoints. To assess the proximity of probe j to a breakpoint, we sum over neighboring probes $\sum_{i=1}^{100}\left(p_{j-i}^{1}-o_{j-i}\right)^{2}+\left(p_{j+i}^{2}-o_{j+i}\right)^{2}$ to aggregate signal within a 201-probe window centered around the specific probe. This value is divided by $\sum_{i=-100}^{100}\left(p_{j+i}^{1}-o_{j+i}\right)^{2}+\left(p_{j+i}^{2}-o_{j+i}\right)^{2}$ to obtain a test statistic t bounded between 0 and 1, with values close to either extreme indicating a putative recombination breakpoint.

Genome-Wide Parentage Plots We examined genome-wide aCGH data to provide an overall comparison between the parents and offspring, in addition to evidence of independent assortment and crossing over in the six parent-offspring trios. *A. flavus* probe data were normalized using Loess normalization but not log2 transformed, as described previously (Olarte *et al.* 2011). We calculated the median of the $\left(p_{j}^{2}-o_{j}\right)^{2}$ in a five-probe window minus the median of the $\left(p_{j}^{1}-o_{j}\right)^{2}$ in the same five-probe window. This statistic measures the similarity of the offspring to each parent in a five-probe window and was plotted for visual display of putative recombination events. Each red dot in the plots represents one probe (see Figure 7), but the plotted value is based on the five-probe window. The plots for each parent-offspring trio show the approximate physical location of each probe on the chromosome and the degree of similarity of the offspring to each parent on the y-axis. For example, a positive difference translates to an offspring showing more similarity to the top parent (*A. flavus*) in the plot while a negative difference suggests that the offspring is more similar to the bottom parent (*A. parasiticus*). To confirm MLST data, loci that

distinguish parents and offspring directly were mapped onto the parentage plot.

Principle Component and Phylogenetic Analysis Phylogenetic and principal component analysis (PCA) was based on single nucleotide polymorphisms (SNPs) in the four MLST loci examined in experimental hybrids and previously sequenced for natural isolates of *A. flavus* L, S_B, S_{BG}, and *A. parasiticus* sampled from populations in Georgia (US), Benin (BE), India (IN), Argentina (AR) and Australia (AU) (G. G. Moore PhD Thesis). We used PCA to distinguish genetic variation due to common ancestry from variation generated in response to adaption to heterogeneous environments. The analysis was performed on two spatial scales: globally (Figure 8a) and within the US alone (Figure 8b). The US sample included representative isolates of *A. flavus* L, S_B, S_{BG},
and *A. parasiticus* sampled from Georgia (GA), Alabama (AL), Arizona (AZ), Texas (TX), Mississippi (MS) and North Carolina (NC). On both geographic scales, we determined the statistically significant axes of variation using methods implemented in EIGENSOFT (Patterson *et al.* 2004; Patterson *et al.* 2006). We used Tibshirani's gap statistic (Tibshirani *et al.* 2001) to identify the optimal number of clusters defined as the subpopulations or subspecies. PCA plots were then extended with phenotypic data (total aflatoxin) to determine the broader species/strain composition of clusters that harbor hybrid progeny. Specifically, we wanted to determine if clades with hybrid progeny that show significant quantitative differences in toxin production from parental species also include natural isolates that have higher total mean aflatoxin concentrations.

To determine the ancestral relationships among clades inferred from PCA analysis

we subjected the four-locus MLST data to maximum likelihood analysis with rapid bootstrapping using RAxML (Stamatakis *et al.* 2008). We performed maximum likelihood bootstrap analysis by specifying distinct partitions for each locus comprising the MLST and assuming different rates of nucleotide substitutions.

RESULTS

Interspecific Crosses Crosses showed quantitative variation in (1) the number of sclerotia/stromata per slant; (2) the proportion of sclerotia/stromata with ascocarps; and (3) the proportion of sclerotia/stromata containing ascospore-bearing ascocarps (Table 1). The percentage of sclerotia/stromata with ascospore-bearing ascocarps ranged from 0 to 33.7 ± 5.9. Of the forty-five attempted crosses, only four produced a measurable number of ascospore-bearing ascocarps (Table 1). The number of sclerotia produced did not correlate with fertility (formation of ascospore-bearing ascocarps), as seen in cross IC278 x IC65, which had the highest fertility but was one of the lower sclerotial producers (Table 1).

Light Microscopy and SEM Following incubation of sclerotia from interspecific matings between *A. flavus* and *A. parasiticus* cultures, we observed indehiscent ascocarps within the matrix of the sclerotium (Figure 2b). The ascocarp wall separated the contents within from the sclerotial tissue (Figures 2d, 2e, 2f). Since the sclerotium acts as a repository for sexual reproductive structures, it is now more appropriately referred to as a stroma. Asci formed within the ascocarps (Figure 2h), and each ascus typically contained eight ascospores. The

ascospores contained a single oil droplet (Figure 2g) and were oblate-shaped, subglobose in face view, finely roughened, and encircled by a distinct equatorial ridge (Figure 2i, 2j). While the general sizes of ascocarps seemed to vary, the stromata were typically found to be between 0.5 mm to 1.0 mm. Ascospores were found to be approximately 6 to 8 µm.

Mycotoxin Quantification and Heritability Mean parental and progeny AFs B_1, B_2, G_1, G_2 and CPA concentrations (µg/mL; n = 3) are shown in Table 2. The calculated heritability (h^2) was 0.7738 ± 0.1768 (95% CI: [0.3919, 1.156]) for AFs B_1+B_2, 0.6543 ± 0.1665 (95% CI: [0.2946, 1.014]) for AFs G_1+G_2 and 0.8371 ± 0.1766 (95% CI: [0.4297, 1.244]) for CPA production (Figure 3); the remaining proportion of the variance for each can be explained by genotype and environment effects. Out of a total of forty-eight assayed progeny, there were seventeen in which B_1 + B_2 AF production was found to be significantly higher than at least one parent; ten hybrid progeny in which G_1 + G_2 AF production was found to be significantly higher than at least one parent; and seven hybrid progeny were found to produce significantly higher amounts of both B and G AF compared to at least one of their respective parents (Table 2). Three progeny (IC1612, IC1622 and IC1630) synthesized G_1 and G_2 aflatoxins that were not produced by the parents. Fourteen hybrid progeny showed significantly higher CPA production than at least one parent. This was based on three biological replicates for each isolate.

MLSTs As confirmed by MLST genotyping, 77% (34/44) of the progeny were recombinants via independent assortment, whereas only one progeny (IC1606) was a

recombinant in the AF gene cluster (Table 2). Unlinked loci segregated in a Mendelian fashion and showed independent assortment. For example, in cross IC278 × IC65, genotyping (Table 2) and aCGH (see Figures 4 and 7b) showed that progeny isolate IC1612 had the genetic background of the *A. flavus* parent IC278 for chromosomes 3, 5 and 6, and inherited chromosomes 4 and 7 of the *A. parasiticus* parent IC65. Putative crossovers in these chromosomes are localized to subtelomeric/telomeric and centromeric regions, giving rise to crossover hybrids as observed in the right arm of chromosome 3 (Figure 7b).

Although there was a statistically significant difference in the frequency of *MAT1-1* (75%) and *MAT1-2* (25%) in the progeny pooled from all crosses (n = 44, $P = 0.0012$), each cross tested separately showed no significant different in frequency of *MAT1-1* versus *MAT1-2*, as is expected for any two segregating loci that are able to assort independently during meiosis. Similarly, we examined segregation of linked AF cluster genes (*aflM/aflN, aflW/aflX,*), *trpC* and *MAT* in each cross, and with the exception of *trpC* in crosses IC278 × IC327 where H2 predominates, there were no significant differences in the frequency of the two parental alleles in the progeny (data not shown).

Heat Maps and Genome-Wide Dendrogram Clustering based on the array data revealed three distinct clades: *A. parasiticus, A. flavus* S strains including experimental hybrids and an *A. flavus* L clade (Figure 4). There was further resolution of Geiser's groups IA, IB, and IC within the *A. flavus* L clade. One experimental hybrid progeny strain IC1630 showed very close similarity to *A. flavus* S. The corresponding heat maps for chromosome 3R are shown in Figure 5. In *A. flavus* L the heat maps show patterns of deletions in the cluster consistent

with Geiser's group IB (Geiser *et al.* 1998), whereas experimental hybrids show a hybridization pattern similar to *A. flavus* S, *A. caelatus*, *A. tamarii* and *A. nomius*.

Parent-Offspring Trio Heat Maps Heat maps of six parent-offspring trios identified putative crossovers in the AF cluster of three progeny based on single feature polymorphisms (SFPs). All three recombinant hybrids in chromosome 3R, IC1612, IC1616 and IC1622, arose from a single crossover in the *aflE* and *aflE/aflM* intergenic region (Figure 6). Because our cluster-specific genetic markers of the MLST are in the *aflM/aflN* and *aflW/aflX* regions these crossovers were only detected using aCGH. All aCGH data were submitted to the Gene Expression Omnibus (GEO) under Accession numbers EED51121.1 - EED51201.1.

Genome-Wide Parentage Plots Both independent assortment and crossovers were observed in genome-wide aCGH parentage plots for the six parent-offspring trios (Figure 7). Sequence data from linked loci in the AF cluster (*aflM/aflN* and *aflW/aflX*) and unlinked loci comprising the MLST (*MAT*, *trpC*) confirmed that patterns of inheritance observed in parentage plots are the result of SFPs between the labeled target DNA hybridized to unlabeled *A. flavus* NRRL 3357 probes fixed on the array. Known patterns of descent from sequenced MLST loci (position indicated with vertical blue lines in parentage plots) confirm inferred independent assortment and crossover events based on array SFP data. For example, the *trpC* sequence on chromosome 4 in progeny IC1612 is identical to the *A. parasiticus* parent IC65, whereas *MAT1-1* on chromosome 6 is from the *A. flavus* parent IC278 (Table 2, Figure 7b).

In the absence of crossovers, chromosomal inheritance in progeny isolates can be deduced by comparing SFPs in parentage plots. An example of this is chromosome 7 in Figure 7d. Notice that all of the detected SFPs occur above the axis, indicating that the entire chromosome is *A. flavus* in genetic background. Frequent crossover events resulted in most progeny having chromosomes of hybrid origin. Crossovers were predominantly located in telomeric/subtelomeric regions. For example, in the AF gene cluster for IC1622, the terminal portion of chromosome 3R is from *A. flavus* parent IC278, while the *aflM/aflN* and *aflW/aflX* regions (leftmost two vertical lines) are from *A. parasiticus* parent IC324, suggesting one crossover in chromosome 3R; the telomeric end of the left arm of chromosome 3 also shows evidence of a crossover but in this case IC1622 is more similar to IC278 (Figure 7d). In some interspecific progeny, crossovers were localized to centromeric regions of chromosomes. For example, IC1630 inherited the right arm of chromosome 5 from the *A. flavus* parent (IC278) and the left arm from the *A. parasiticus* parent (IC324). In IC1616 and IC1603, crossovers coincide with the putative location of centromeres on chromosomes 5 and 1, respectively.

The *A. flavus* oligonucleotide-based microarrays allow recombination breakpoint resolution of approximately 15 kb based on the spacing of probes between adjacent genes. The higher probe density in the tiled intergenic regions of the AF cluster provided higher breakpoint resolution; the dissimilarity between *A. parasiticus* and the *A. flavus* oligonucleotide-based probes on the arrays further enhanced breakpoint resolution genome-wide. Overall at least one crossover per chromosome arm was observed with double and triple crossovers more common on longer chromosome arms, for example, chromosome 1R.

Principle Component and Phylogenetic Analysis PCA identified a total of three significant axes of variation in the global MLST data. The first two axes partitioned the isolates into clusters of *A. parasiticus* and *A. flavus* L strain as well as a distinct combined *A. flavus* S_B and S_{BG} group of strains from Australia and Benin. Examining a third significant axis of variation revealed a separate cluster of *A. flavus* S_{BG} isolates from Benin. Applying Tibshirani's gap statistic (Tibshirani *et al.* 2001) on the PCA of the three axes revealed at least three significant clusters: *A. parasiticus, A. flavus* L and *A. flavus* S_B/S_{BG}. Experimental hybrids were tightly clustered with natural isolates sampled from populations in Georgia (US), Benin (BE), India (IN), Argentina (AR) and Australia (AU).

Maximum likelihood bootstrap analysis revealed three distinct paraphyletic *A. flavus* L-strain clades and one large monophyletic *A. parasiticus* clade (see Figure 8A); *A. flavus* S_B- and S_{BG}–strains share a recent common ancestor in Australia and Argentina but the S_{BG}– strains form a distinct monophyletic group in Benin. The hybrid strains share haplotypes with *A. parasiticus* (haplotypes H1 and H154) and *A. flavus* L (haplotypes H113 and H155); haplotype 155 and hybrid haplotype H162 also share a recent common ancestor with *A. flavus* S_{BG} (haplotypes H85, H90 and H160).

DISCUSSION

We present the first direct genetic evidence of interspecific hybridization between *A. flavus* and *A. parasiticus*. We also show that interspecific hybrids show heterosis in aflatoxin

production; further, there was also evidence of heterosis associated with CPA production. Several mechanisms may be involved that increase aflatoxin concentrations in hybrid progeny. One possibility is variation in patterns of DNA methylation in the aflatoxin gene cluster and genome-wide. DNA methylation contributes to epigenetic processes, which play a fundamental role in organismal adaptation to different environmental conditions (Angers *et al.* 2010). Because DNA methylation signatures are transmitted across generations and are highly heritable, modifications of these patterns as a result of crossovers and independent assortment may relieve or activate repressors or other regulators of aflatoxin production. For example, hybrid offspring IC1603 and IC1637 have significantly higher and lower mean aflatoxin B1 concentrations, respectively, than the parental *A. flavus* IC278 strain. In both IC1603 and IC1637 there is no evidence of crossovers in the aflatoxin cluster, which suggests that the factors modulating toxicity are located elsewhere in the genome. The possibility of using interspecific crosses for genetic mapping of loci that down- and un-regulate toxicity warrants further investigation.

The high heritability of both AF and CPA in interspecific crosses indicates that genetic variation, in the form of mutations and recombination, has a direct effect on toxin diversity. Recombination as a result of hybridization may be important in the genesis of unique hybrid toxin profiles. For example, two progeny (IC1612, and IC1622) synthesized G_1 and G_2 aflatoxins that were not produced by the parents. In both cases gain of G aflatoxin function was the result of a crossover event between *A. flavus* (IC278) and *A. parasiticus* (IC65 or IC324) in the midpoint segment of the cluster close to *aflE* (Figure 6), such that the

region from *aflE* to the telomere was inherited from the OMST producing *A. parasiticus* parent. This indicates that the loss of function
mutation in these OMST producing *A. parasticus* strains is somewhere in the *aflE-nadA* late pathway segment of the cluster. A recent study reports that *ordA* (=*aflQ*), *cypA*(=*aflU*) and *nadA* are important in the conversion of OMST to G aflatoxins (Zeng *et al.* 2011). Since *aflU* is in the *A. parasiticus* telomeric segment this suggests that *aflU* is functional in IC1612 and IC1622 and that the possible loss of function mutations reside in *aflO, nadA,* or both. Other crossover events that result in the inheritance of the telomeric end from the *A. flavus* parent results in hybrid progeny that produce B and G aflatoxins as well as CPA. The only putative example, originating from the same cross as IC1622 (Table 2), is IC1630 but we would expect to detect more progeny with a similar toxin profile with a larger sampling of offspring.

According to the genotyping results (Table 2), with the exception of *MAT,* IC1630 shares the same multilocus haplotype as parental strain IC324 with no evidence of a crossover in the aflatoxin cluster (Figure 6) so we would expect strain IC1630 to make OMST and no CPA; however it synthesizes B and G aflatoxins, as well as CPA. The trio heat map of IC278, IC1630 and IC324 (Figure 6) revealed a unique hybridization phenotype for IC1630 similar to that observed for strains of *A. flavus* S, *A. nomius, A. tamari,* and *A. caelatus* (Figure 5). A closer inspection of the corresponding aCGH parentage plot of this trio shows high hybridization signal intensity in the subtelomeric segment of chromosome 3R (Figure 7E) that is in the direction of both parents, particularly in the telomeric end. This signature was not observed elsewhere in the genome of IC1630 and there was no evidence of

this phenotype in the heat maps of chromosome 3R of other hybrid progeny (Figure 5). A similar phenomenon was observed in *A. flavus* intraspecific crosses (Olarte *et al.* 2011) where it was interpreted as the existence of genetically heterogeneous nuclei that are heterokaryotic for the aflatoxin gene cluster. We hypothesize that the nuclei are genetically unbalanced with respect to the right arm of chromosome 3, and as a result the cluster copy number is lower than adjacent regions. Clearly the toxin phenotype data indicate that a crossover occurred between the aflatoxn clusters of *A. flavus* and *A. parasiticus* but the resultant recombinant is present in less than single copy levels making it difficult to resolve using aCGH. Examining additional genetic markers in the aflatoxin and CPA clusters of IC1630 may further elucidate the recombination structure of this hybrid offspring. This work is currently in progress. Whether copy variation in the cluster plays a role in regulating aflatoxin biosynthesis and facilitating adaptation in these fungi warrants further investigation. These data indicate that there may be several different mechanisms that generate toxin diversity in these fungi.

The nuclear condition of these fungi may also impact their fertility. As reported previously in *A. parasiticus* (Horn *et al.* 2009b) and *A. flavus* (Horn *et al.* 2009a), the same parental strain in different crosses yielded different fertilities. For example, *A. parasiticus* IC65 had the highest fertility when crossed with *A. flavus* IC278 and the lowest fertility when crossed to IC314 (Table 1). In this study, it appeared that the *A. flavus* parental strain drove fertility in interspecific crosses. Previous work indicated that IC65 was possibly heterokaryotic for mating type (Carbone, unpublished data). Whether heterokaryosis plays a role in fertility is unknown and warrants further investigation.

Results from PCA and phylogenetic analysis suggest that hybrid offspring are polyphyletic showing tight clustering and common ancestry with *A. flavus* L- and S- strains and *A. parasiticus.* The clustering of S_B and S_{BG} isolates suggests either recent population admixture or the possible existence of polymorphisms that associate with environmental heterogeneity. Furthermore, hybrid progeny strains appear to cluster with chemotype specific toxin classes within each species/morphotype. For example, hybrid progeny IC1630, which produces B and G aflatxoins and CPA groups with IC1112, an *A. flavus* S strain from Benin with a similar toxin profile. This clustering is only observed in the dendrogram, which is based on genome-wide SFPs. In the maximum likelihood DNA-sequence based phylogeny IC1630 shares a haplotype with other naturally occurring *A. parasiticus* OMST producers, which suggests clonal expansion or selection acting to maintain this chemotype-specific class, as reported previously (Carbone *et al.* 2007b). In the study by Carbone and coworkers (2007), the *hypE* gene located in the *aflM/aflN* intergenic region was shown to be target of balancing selection acting to maintain G_1-dominant and OMST specific classes in *A. parasiticus.* The recently shared common ancestry of *A. parasticus* G_1 dominant strains and *A. flavus* based on variation in *hypE* supports the possibility of interspecific hybridization giving rise to G_1 dominant strains in *A. parasiticus.* PCA analysis in Figure 8 shows that hybrids are positioned at extremes within each *A. parasiticus* and *A. flavus* species cluster, which indicates that they may contribute to the genetic and toxin heterogeneity observed in natural populations. For example, super aflatoxin-producing (600-1000μg/mL) hybrid progeny IC1602 and IC1643 are tightly clustered with high aflatoxin producing *A. parasiticus* and *A. flavus* strains sampled from nature. Further examination of interspecific

hybrids may yield additional insights into the evolution of toxicity in these agriculturally important species.

REFERENCES

Abbas HK, Zablotowicz RM, Horn BW, *et al.* (2011) Comparison of major biocontrol strains of non-aflatoxigenic *Aspergillus flavus* for the reduction of aflatoxins and cyclopiazonic acid in maize. *Food Additives and Contaminants* **28**, 198-208.

Angers B, Castonguay E, Massicotte R (2010) Environmentally induced phenotypes and DNA methylation: how to deal with unpredictable conditions until the next generation and after. *Molecular Ecology* **19**, 1283-1295.

Aylor DL, Price EW, Carbone I (2006) SNAP: combine and map modules for multilocus population genetic analysis. *Bioinformatics* **22**, 1399-1401.

Bigelow DM, Orum TV, Cotty PJ, Nelson MR (2001) Monitoring Aspergillus flavus AF36 and S strain incidence in the Desert Southwest. *Phytopathology* **91**, S181-S182.

Brasier C (2000) The rise of the hybrid fungi. *Nature* **405**, 134-135.

Burdock GA, Flamm WG (2000) Safety assessment of the mycotoxin cyclopiazonic acid. *International Journal of Toxicology* **19**, 195–218.

Carbone I, Jakobek JL, Ramirez-Prado JH, Horn BW (2007a) Recombination, balancing selection and adaptive evolution in the aflatoxin gene cluster of *Aspergillus parasiticus*. *Molecular Ecology* **16**, 4401–4417.

Carbone I, Ramirez-Prado JH, Jakobek JL, Horn BW (2007b) Gene duplication, modularity and adaptation in the evolution of the aflatoxin gene cluster. *BMC Evolutionary Biology* **7**, 111.

Chang P-K, Horn BW, Dorner JW (2005) Sequence breakpoints in the aflatoxin biosynthesis gene cluster and flanking regions in nonaflatoxigenic *Aspergillus flavus* isolates. *Fungal Genetics and Biology* **42**, 914-923.

Coppin E, Debuchy R, Arnaise S, Picard M (1997) Mating types and sexual development in filamentous ascomycetes. *Microbiol Mol. Biol. Rev.* **61**, 411–428.

Cotty PJ (1989) Virulence and cultural characteristics of two *Aspergillus flavus* strains pathogenic on cotton. *Phytopathology* **79**, 808-814.

Dorner JW (2005) Biological control of aflatoxin crop contamination. In: *Aflatoxin and Food Safety* (ed. Abbas HK), pp. 333–352. Taylor and Francis, Boca Raton, Florida.

Ehrlich KC (2008) Genetic diversity in *Aspergillus flavus* and its implications for agriculture. In: *Aspergillus in the genomic era* (eds. Varga J, Samson RA), pp. 233-247. Wageningen Academic Publishers, Wageningen, Netherlands.

Ehrlich KC, Kobbeman K, Montalbano BG, Cotty PJ (2007) Aflatoxin-producing Aspergillus species from Thailand. *Int J Food Microbiol* **114**, 153-159.

Fazekas B, Tar A, Kovacs M (2005) Aflatoxin and ochratoxin A content of spices in Hungary. *Food Additives and Contaminants* **22**, 856-863.

Fedorova ND, Harris S, Chen D, *et al.* (2009) Using aCGH to study intraspecific genetic variability in two pathogenic molds, *Aspergillus fumigatus* and *Aspergillus flavus*. *Medical Mycology* **47**, S34-S41.

Frisvad JC, Skouboe P, Samson RA (2005) Taxonomic comparison of three different groups of aflatoxin producers and a new efficient producer of aflatoxin B-1,

sterigmatocystin and 3-O-methylsterigmatocystin, *Aspergillus rambellii* sp nov. *Systematic and Applied Microbiology* **28**, 442-453.

Geiser DM, Pitt JI, Taylor JW (1998) Cryptic speciation and recombination in the aflatoxin-producing fungus *Aspergillus flavus*. *Proceedings of the National Academy of Sciences, USA* **95**, 388-393.

Gieseker KE, Nyikal J, Misore A*, et al.* (2004) Outbreak of aflatoxin poisoning--eastern and central provinces, Kenya, January-July 2004. *Faculty Publications* **53**, 790-793.

Godet M, Munaut F (2009) Molecular strategy for identification in *Aspergillus* section *Flavi*. *FEMS Microbiol. Lett.* **304**, 157-168.

Gross BL, Riesberg LH (2005) The ecological genetics of homoploid hybrid speciation. *Journal of Heredity* **96**, 241-252.

Hedayati MT, Pasqualotto AC, Warn PA, Bowyer P, Denning DW (2007) *Aspergillus flavus*: human pathogen, allergen and mycotoxin producer. *Microbiology* **153**, 1677-1692.

Hendry AP (2009) Speciation. *Nature* **458**, 162-164.

Horn BW (2005) Ecology and population biology of aflatoxigenic fungi in soil. In: *Aflatoxin and Food Safety* (ed. Abbas HK), pp. 95-116. CRC Taylor & Francis, Boca Raton.

Horn BW, Dorner JW (1999) Regional differences in production of aflatoxin B_1 and cyclopiazonic acid by soil isolates of *Aspergillus flavus* along a transect within the United States. *Applied and Environmental Microbiology* **65**, 1444-1449.

Horn BW, Greene RL (1995) Vegetative compatibility within populations of *Aspergillus flavus, Aspergillus parasiticus,* and *A. tamarii* from a peanut field. *Mycologia* **87**, 324-332.

Horn BW, Greene RL, Sobolev VS*, et al.* (1996) Association of morphology and mycotoxin production with vegetative compatibility groups in *Aspergillus flavus, A. parasiticus,* and *A. tamarii*. *Mycologia* **88**, 574–587.

Horn BW, Moore GG, Carbone I (2009a) Sexual reproduction in *Aspergillus flavus*. *Mycologia* **101**, 423-429.

Horn BW, Moore GG, Carbone I (2011) Sexual reproduction in aflatoxin-producing *Aspergillus nomius*. *Mycologia* **103**, 174-183.

Horn BW, Ramirez-Prado JH, Carbone I (2009b) Sexual reproduction and recombination in the aflatoxin-producing fungus *Aspergillus parasiticus*. *Fungal Genetics and Biology* **46**, 169-175.

Horn BW, Ramirez-Prado JH, Carbone I (2009c) The sexual state of *Aspergillus parasiticus*. *Mycologia* **101**, 275-280.

Klich MA (2007) Aspergillus flavus: the major producer of aflatoxin. *Molecular Plant Pathology* **8**, 10.

Lamb MC, Sternitzke DA (2001) Cost of aflatoxin to the farmer, buying point, and sheller segments of the southeast United States peanut industry. *Peanut Science* **28**, 59-63.

Mallet J (2007) Hybrid speciation. *Nature* **446**, 279-283.

McAlpin CE, Wicklow DT (2005) Culture media and sources of nitrogen promoting the formation of stromata and ascocarps in *Petromyces alliaceus* (*Aspergillus* section *Flavi*). *Can. J. Microbiol.* **51**, 765–771.

Moore GG, Singh R, Horn BW, Carbone I (2009) Recombination and lineage-specific gene loss in the aflatoxin gene cluster of *Aspergillus flavus*. *Molecular Ecology* **18**, 4870-4887.

Olarte RA, Horn BW, Dorner JW*, et al.* (2011) Effect of sexual recombination on population diversity in alfatoxin production by *Aspergillus flavus* and evidence for cryptic heterokaryosis. *Molecular Ecology* **In Press**.

Papa KE (1986) Heterokaryon incompatibility in Aspergillus flavus. *Mycologia* **78**, 98-101.

Patterson N, Hattangadi N, Lane B*, et al.* (2004) Methods for high-density admixture mapping of disease genes. *American Journal of Human Genetics* **74**, 979-1000.

Patterson N, Price AL, Reich D (2006) Population structure and eigenanalysis. *PLoS Genetics* **3**, 2074-2093.

Payne GA (1998) Process of contamination by aflatoxin-producing fungi and their impact on crops. In: *Mycotoxins in Agriculture and Food Safety* (eds. Sinha KK, Bhatnagar D), pp. 279–306. Marcel Dekker, New York.

Payne GA, Yu J, Nierman WC*, et al.* (2008) A first glance into the genome sequence of *Aspergillus flavus*. In: *The Aspergilli : genomics, medical aspects, biotechnology, and research methods* (eds. Osmani SA, Goldman GH), pp. 15-23. CRC Press, Boca Raton.

Peterson SW, Ito Y, Horn BW, Goto T (2001) *Aspergillus bombycis,* a new aflatoxigenic species and genetic variation in its sibling species, *A. nomius*. *Mycologia* **93**, 689-703.

Pildain MB, Frisvad JC, Vaamonde G, *et al.* (2008) Two novel aflatoxin-producing *Aspergillus* species from Argentinean peanuts. *Int J Syst Evol Microbiol* **58**, 725-735.

Pitt JI (2000) Toxigenic fungi: which are important? *Med Mycol* **38**, 17-22.

Price EW, Carbone I (2005) SNAP: workbench management tool for evolutionary population genetic analysis. *Bioinformatics* **21**, 402-404.

Probst C, Njapau H, Cotty PJ (2007) Outbreak of an acute aflatoxicosis in Kenya in 2004: Identification of the causal agent. *Applied and Environmental Microbiology* **73**, 2762-2764.

R Development Core Team (2010) R: A language and environment for statistical computing. R Foundation for Statistical Computing, Vienna, Austria.

Ramirez-Prado JH, Moore GG, Horn BW, Carbone I (2008) Characterization and population analysis of the mating-type genes in *Aspergillus flavus* and *Aspergillus parasiticus*. *Fungal Genetics and Biology* **45**, 1292-1299.

Raper KB, Fennell DI (1965) *The genus Aspergillus* Williams and Wilkins, Baltimore, Maryland.

Schardl CL, Craven KD (2003) Interspecific hybridization in plant-associated fungi and oomycetes: a review. *Molecular Ecology* **12**, 2861-2873.

Schwenk K, Brede N, Streit B (2008) Extent, processes and evolutionary impact of interspecific hybridization in animals. *Phil. Trans. R. Soc. B* **363**, 2805-2811.

Stamatakis A, Hoover P, Rougemont J (2008) A rapid bootstrap algorithm for the RAxML web servers. *Systematic Biology* **57**, 758-771.

Tibshirani R, Walther G, Hastie T (2001) Estimating the number of clusters in a data set via the gap statistic. *Journal of the Royal Statistical Society Series B-Statistical Methodology* **63**, 411-423.

Vardon P, McLaughlin C, Nardinelli C (2003) Potential economic costs of mycotoxins in the United States. In: *Council for Agricultural Science and Technology (CAST). Mycotoxins: Risks in Plant, Animal, and Human Systems*, Ames, IA.

Zeng H, Hatabayashi H, Nakagawa H*, et al.* (2011) Conversion of 11-hydroxy-O-methylsterigmatocystin to aflatoxin G1 in Aspergillus parasiticus. *Applied Microbial and Cell Physiology* **90**, 635-650.

Table 1. Incidences of sexual state in forty-five attempted interspecific crosses between compatible mating types of *Aspergillus flavus and A. parasiticus*

MAT 1-1[1]			*MAT1-2*[1]			Number of sclerotia/stromata per slant[4]	Number of sclerotia/stromata examined	% with ascocarps[4,5]	% with ascospore-bearing ascocarps[4,6]
IC strain	NRRL strain[2]	VCG[3]	IC strain	NRRL strain[2]	VCG[3]				
A. flavus x *A. parasiticus*									
IC289	29518	44	IC69	-	10	0	-	-	-
IC314	-	-	IC65	29602	8	24 ± 17	113	0	-
IC314	-	-	IC33	29570	3	47 ± 21	237	0	-
IC283	29512	38	IC67	-	9	47 ± 30	234	0	-
IC289	29518	44	IC324	35779	-	83 ± 37	376	0	-
IC314	-	-	IC324	35779	-	121 ± 49	309	0	-
IC308	29537	63	IC59	-	6	398 ± 63	300	0	-
IC283	29512	38	IC65	29602	8	623 ± 114	300	0	-
IC289	29518	44	IC65	29602	8	627 ± 196	300	0	-
IC283	29512	38	IC324	35779	-	669 ± 50	300	0	-

Table 1 Continued

IC283	29512	38	IC329	35784	-	710 ± 6	300	0	-
IC289	29518	44	IC330	35785	-	221 ± 46	300	0.7 ± 1.1	0
IC308	29537	63	IC65	29602	8	418 ± 30	300	0.7 ± 1.1	0
IC311	-	-	IC331	35786	-	1650 ± 101	300	2.7 ± 1.1	0
IC311	-	-	IC324	35779	-	1225 ± 11	300	6.3 ± 3.2	0
IC311	-	-	IC65	29602	8	1053 ± 36	300	8.7 ± 4.0	0
IC311	-	-	IC72	-	13	613 ± 68	300	12.7 ± 0.6	0
IC308	29537	63	IC324	35779	-	891 ± 42	300	0.3 ± 0.6	0.3 ± 0.6
IC308	29537	63	IC328	35783	-	635 ± 14	300	1.0 ± 1.0	0.7 ± 0.6
IC278	29507	33	IC33	29570	3	232 ± 66	300	12.3 ± 5.0	6.0 ± 2.6
IC278	29507	33	IC327	35782	-	324 ± 32	420	28.4 ± 9.3	10.6 ± 3.9
IC278	29507	33	IC324	35779	-	398 ± 59	400	36.3 ± 9.2	26.7 ± 6.5
IC278	29507	33	IC65	29602	8	282 ± 133	300	49.7 ± 7.0	33.7 ± 5.9
A. parasiticus x *A. flavus*									
IC61	-	7	IC1179	AF36	-	4 ± 8	20	0	-
IC1	-	1	IC1179	AF36	-	8 ± 4	40	0	-
IC73	-	14	IC1179	AF36	-	23 ± 12	115	0	-

Table 1 Continued

IC49	-	4	IC1179	AF36	-	33 ± 14	164	0	-
IC65	-	8	IC271	29500	28	37 ± 14	147	0	-
IC49	-	4	IC229	29459	6	62 ± 42	283	0	-
IC65	-	8	IC309	-	-	71 ± 57	289	0	-
IC65	-	8	IC1179	AF36	-	126 ± 26	306	0	-
IC73	-	14	IC201	21882	24	674 ± 98	300	0	-
IC65	-	8	IC201	21882	24	1184 ± 351	300	0	-
IC65	-	8	IC277	29506	32	1430 ± 96	300	0	-
IC74	-	15	IC201	21882	24	736 ± 49	300	0.3 ± 0.6	0
IC65	-	8	IC229	29459	6	484 ± 142	300	1.0 ± 1.7	0
IC75	-	16	IC229	29459	6	18 ± 9	90	1.1 ± 2.5	0
IC73	-	14	IC229	29459	6	186 ± 111	300	1.3 ± 0.6	0
IC49	-	4	IC201	21882	24	689 ± 87	300	2.0 ± 1.7	0
IC53	-	5	IC229	29459	6	12 ± 7	58	2.0 ± 4.5	0
IC44	-	4	IC201	21882	24	677 ± 129	300	3.0 ± 2.0	0
IC73	-	14	IC202	29506	-	734 ± 40	300	4.0 ± 3.6	0
IC18	-	2	IC202	29506	-	610 ± 114	300	7.7 ± 4.2	0
IC49	-	4	IC277	29506	32	806 ± 40	300	12.3 ± 3.5	0
IC70	-	11	IC202	29506	-	632 ± 148	300	19.0 ± 3.6	0

Table 1 Continued

[1]Mating-type designations for NRRL strains: 29507, 29570, 35782 from Ramirez-Prado *et al*. (2008).

[2]Strain numbers (NRRL) from Agricultural Research Service Culture Collection, Peoria, Illinois, USA. Strains with an unassigned NRRL are indicated with a '-'.

[3]Vegetative compatibility groups based on Horn and Greene (1995). Strains of unknown VCG are indicated with a '-'.

[4]Means ± s.d. (*n* = 3-5 culture slants or biological replicates).

[5]Percentage of total number of sclerotia/stromata examined containing one or more ascocarps irrespective of the presence of ascospores.

[6]Percentage of total number of sclerotia/stromata examined containing one or more ascospore-bearing ascocarps

Table 2. Multilocus genotypes and mycotoxin phenotypes from four most fertile interspecific crosses between *Aspergillus flavus* and *A. parasiticus*.

IC Strain	Loci examined[a]				OMST[d]	Aflatoxin[c]						CPA (μg/mL)[e]	Cluster MLST[f]	Genome MLST[g]
	Chr. 6 *MAT*	Chr. 3 *aflM*	Chr. 3 *aflW*	Chr. 4 *trpC*	(μg/mL)	B_1 (μg/mL)	B_2 (μg/mL)	G_1 (μg/mL)	G_2 (μg/mL)	Total Bs (μg/mL)	Total Gs (μg/mL)			
Parents														
IC278	1	H1	H1	H1	1.4 (0.7)	119.0 (51.1)	3.1 (1.7)	0 (0)	0 (0)	122.1 (52.7)	0 (0)	140.5 (4.2)	H1	H1
IC327	2	H2	H2	H2	0.2 (0.0)	210.9 (42.4)	9.9 (2.1)	169.5 (28.9)	4.2 (0.8)	220.8 (44.5)	173.7 (29.8)	0 (0)	H2	H2
Progeny														
Ascocarp 1[h]														
IC1596	1	H1	H1	H1	0.4 (0.1)	23.1 (12.8)	0.5 (0.3)	0 (0)	0 (0)	23.6 (13.1)**	0 (0)**	18.2 (6.9)*	H1	H1
IC1597	2	H1	H1	H2	0.1 (0.1)	20.9 (7.6)	0.3 (0.1)	0 (0)	0 (0)	21.2 (7.8)**	0 (0)**	91.3 (39.8)***	H1	H3
Ascocarp 2														
IC1598	1	H2	H2	H2	1.0 (0.4)	127.0 (18.5)	3.1 (0.8)	143.2 (50.8)	2.3 (1.1)	130.1 (18.9)	145.5 (51.9)	0 (0)*	H2	H4

Table 2 Continued

IC1599	1	H2	H2	H2	1.4 (0.5)	347.1 (24.4)	10.9 (0.7)	234.4 (7.8)	4.7 (0.1)	358.0 (25.1)***	239.1 (7.89)*	0 (0)*	H2	H4
IC1600	1	H2	H2	H2	1.7 (0.2)	281.6 (100.2)	10.3 (5.2)	201.7 (102.3)	4.6 (2.7)	291.9 (105.4)*	206.4 (105.0)*	0 (0)*	H2	H4
IC1601	1	H2	H2	H2	1.2 (0.6)	136.5 (31.9)	5.6 (1.0)	184.2 (15.8)	4.4 (0.8)	142.1 (32.8)	188.7 (15.7)*	0 (0)*	H2	H4
Ascocarp 3														
IC1602	2	H2	H2	H2	1.7 (0.5)	353.9 (53.6)	16.8 (4.5)	583.9 (132.2)	16.0 (6.1)	370.7 (57.5)***	599.9 (138.2)***	0 (0)*	H2	H2
IC1603	1	H1	H1	H2	0.5 (0.1)	209.8 (29.2)	7.5 (1.5)	0 (0)	0 (0)	217.3 (30.6)	0 (0)**	130.6 (21.0)**	H1	H6
IC1604	1	H2	H2	H2	2.3 (1.6)	127.9 (38.8)	5.9 (2.0)	260.6 (62.4)	6.4 (2.1)	133.8 (40.8)	266.9 (64.5)*	0 (0)*	H2	H4
IC1605	1	H2	H2	H2	1.1 (0.1)	225.4 (10.0)	9.2 (0.9)	362.2 (17.2)	10.0 (1.0)	234.6 (10.8)	372.1 (17.8)***	0 (0)*	H2	H4
IC1606	1	H3	H1	H2	1.3 (0.1)	315.8 (6.9)	12.1 (0.5)	0 (0)	0 (0)	328.0 (7.4)*	0 (0)**	225.5 (8.6)***	H3	H5
IC1607	2	H2	H2	H2	2.2 (0.7)	351.0 (49.4)	13.5 (1.7)	390.6 (37.9)	8.3 (0.7)	364.5 (51.0)***	398.9 (38.6)***	0 (0)*	H2	H2
Parents														
IC278	1	H1	H1	H1	1.5 (0.7)	91.0 (39.5)	2.2 (1.0)	0 (0)	0 (0)	93.2 (40.5)	0 (0)	121.4 (19.0)	H1	H1
IC65	2	H2	H2	H2	346.3 (56.4)	0 (0)	0 (0)	0 (0)	0 (0)	0 (0)	0 (0)	0 (0)	H2	H2

Table 2 Continued

Progeny Ascocarp 1														
IC1608	1	H1	H1	H1	0.8 (0.3)	78.2 (20.9)	1.6 (0.4)	0 (0)	0 (0)	79.8 (21.2)**	0 (0)	80.6 (7.3)***	H1	H3
IC1610	2	H1	H1	H1	1.6 (0.4)	82.6 (24.3)	2.0 (0.7)	0 (0)	0 (0)	84.6 (25.0)**	0 (0)	47.8 (3.8)***	H1	H4
IC1611	1	H2	H2	H2	314.2 (37.5)	0 (0)	0 (0)	0 (0)	0 (0)	0 (0)*	0 (0)	0 (0)*	H2	H6
IC1612	1	H1	H1	H2	3.5 (0.8)	106.9 (14.9)	5.0 (0.7)	164.2 (12.6)	4.9 (0.3)	111.8 (15.6)**	169.1 (12.9)***	0 (0)*	H1	H8
IC1613	1	H2	H2	H1	403.1 (18.9)	0 (0)	0 (0)	0 (0)	0 (0)	0 (0)*	0 (0)	0 (0)*	H2	H7
IC1614	1	H1	H1	H1	0.1 (0.1)	2.5 (1.2)	0 (0)	0 (0)	0 (0)	2.5 (1.2)*	0 (0)	20.4 (3.5)*	H1	H1
IC1615	1	H2	H2	H2	283.6 (18.2)	0 (0)	0 (0)	0 (0)	0 (0)	0 (0)*	0 (0)	0 (0)*	H2	H6
IC1616	1	H2	H2	H2	108.7 (65.6)	0 (0)	0 (0)	0 (0)	0 (0)	0 (0)*	0 (0)	138.1 (28.3)**	H2	H6
IC1617	2	H2	H2	H2	396.2 (6.5)	0 (0)	0 (0)	0 (0)	0 (0)	0 (0)*	0 (0)	0 (0)*	H2	H2
IC1618	2	H1	H1	H2	0.4 (0.3)	202.6 (59.2)	6.7 (2.0)	0 (0)	0 (0)	209.3 (61.0)***	0 (0)	91.4 (16.6)**	H1	H5
IC1619	1	H2	H2	H1	110.6 (73.5)	0 (0)	0 (0)	0 (0)	0 (0)	0 (0)*	0 (0)	30.4 (26.6)*	H2	H7

Table 2 Continued

Parents														
IC278	1	H1	H1	H1	3.0 (1.3)	62.9 (39.3)	1.5 (1.2)	0 (0)	0 (0)	64.4 (40.5)	0 (0)	140.2 (7.4)	H1	H1
IC324	2	H2	H2	H2	310.2 (26.3)	0 (0)	0 (0)	0 (0)	0 (0)	0 (0)	0 (0)	0 (0)	H2	H2
Progeny														
Ascocarp 1														
IC1620	1	H1	H1	H2	2.2 (1.7)	43.9 (20.0)	0.7 (0.2)	0 (0)	0 (0)	44.7 (20.2)	0 (0)	74.0 (40.0)	H1	H3
Ascocarp 2														
IC1622	1	H1	H1	H2	10.8 (1.6)	133.6 (38.9)	9.2 (2.9)	433.9 (110.5)	20.6 (5.5)	142.8 (41.8)**	454.5 (116.0)***	0 (0)*	H1	H3
Ascocarp 3														
IC1623	2	H1	H1	H2	1.6 (0.4)	418.2 (26.2)	18.8 (1.3)	0 (0)	0 (0)	437.0 (27.6)***	0 (0)	249.0 (12.6)**	H1	H4
IC1624	1	H2	H2	H1	218.7 (31.0)	0 (0)	0 (0)	0 (0)	0 (0)	0 (0)	0 (0)	0 (0)*	H2	H6
IC1625	2	H2	H2	H11	122.4 (9.1)	0 (0)	0 (0)	0 (0)	0 (0)	0 (0)	0 (0)	0 (0)*	H2	H5
Ascocarp 4														
IC1626	1	H2	H2	H2	0 (0)	4.5 (2.8)	0.1 (0.1)	0 (0)	0 (0)	4.5 (2.9)	0 (0)	75.4 (11.1)	H2	H7
IC1627	1	H1	H1	H1	4.1 (0.8)	168.0 (78.4)	6.1 (3.0)	0 (0)	0 (0)	174.1 (81.4)***	0 (0)	184.2 (1.4)**	H1	H1

Table 2 Continued

IC1628	1	H1	H1	H1	3.3 (0.7)	257.1 (14.6)	9.5 (0.7)	0 (0)	0 (0)	266.5 (15.3)***	0 (0)	166.7 (27.9)**	H1	H3
Ascocarp 5														
IC1629	1	H1	H1	H1	0.5 (0.1)	173.1 (18.4)	8.3 (1.2)	0 (0)	0 (0)	181.4 (19.5)***	0 (0)	128.5 (10.0)**	H1	H1
IC1630	1	H2	H2	H2	2.3 (0.9)	76.8 (38.5)	2.3 (1.8)	32.5 (29.8)	0.8 (0.9)	79.2 (40.3)	33.3 (30.6)	212.5 (102.1)**	H2	H7
IC1631	2	H2	H2	H1	389.6 (28.6)	0 (0)	0 (0)	0 (0)	0 (0)	0 (0)	0 (0)	0 (0)*	H2	H5
Parents														
IC278	1	H1	H1	H1	3.1 (1.2)	114.8 (34.2)	3.7 (1.9)	0 (0)	0 (0)	118.4 (36.1)	0 (0)	183.0 (26.1)	H1	H1
IC33	2	H2	H2	H2	1.3 (0.3)	47.0 (10.2)	1.5 (0.1)	46.4 (5.3)	0.9 (0.2)	48.4 (10.2)	47.3 (5.4)	0 (0)	H2	H2
Progeny														
Ascocarp 1														
IC1632	2	H2	H2	H2	1.6 (1.2)	52.6 (5.8)	1.2 (0.2)	52.3 (4.4)	0.7 (0.1)	53.8 (6.0)	53.0 (4.5)	0 (0)*	H2	H2
IC1633	1	H2	H2	H2	1.6 (0.9)	217.7 (95.0)	9.0 (6.1)	257.8 (161.7)	6.7 (5.1)	226.7 (100.8)**	264.5 (166.8)	0 (0)*	H2	H3
IC1634	2	H1	H1	H1	2.8 (0.4)	558.7 (66.5)	22.7 (2.9)	0 (0)	0 (0)	581.4 (69.3)***	0 (0)	183.5 (22.4)**	H1	H6

Table 2 Continued

Ascocarp 2														
IC1637	1	H1	H1	H2	0 (0)	12.1 (7.3)	0.2 (0.1)	0 (0)	0 (0)	12.3 (7.4)	0 (0)	34.2 (8.4)*	H1	H4
IC1638	1	H2	H2	H2	5.7 (7.6)	221.8 (155.3)	5.0 (5.4)	206.0 (299.2)	3.5 (5.1)	226.8 (160.7)**	209.6 (304.3)	0 (0)*	H2	H3
IC1639	1	H2	H2	H1	9.7 (1.6)	403.9 (41.5)	11.0 (0.5)	210.6 (5.9)	3.9 (0.3)	414.9 (41.6)***	214.5 (5.7)	0 (0)*	H2	H5
IC1640	1	H2	H2	H2	1.5 (0.4)	83.1 (9.6)	2.5 (0.8)	107.5 (42.1)	2.1 (1.1)	85.6 (10.3)	109.5 (43.2)	0 (0)*	H2	H3
IC1641	1	H1	H1	H2	3.9 (1.7)	74.0 (24.9)	1.4 (0.3)	0 (0)	0 (0)	75.4 (25.2)	0 (0)	122.5 (9.4)***	H1	H4
IC1642	1	H2	H2	H2	0.8 (0.2)	82.8 (14.9)	1.5 (0.1)	48.9 (10.3)	0.7 (0.1)	84.3 (15.0)	49.6 (10.4)	0 (0)*	H2	H3
IC1643	1	H2	H2	H1	2.6 (1.8)	257.0 (34.9)	10.2 (0.9)	516.9 (72.9)	12.4 (1.4)	267.2 (35.8)**	529.3 (74.3)***	0 (0)*	H2	H5

[a]Parental mating-type (*MAT*) designations for NRRL strains 29602, 35779 and 35782 are from Ramirez-Prado *et al*. (2008); parental mating-type (*MAT*) designations for NRRL strains 29507 and 29570 are from Horn *et al*. (2009).

[b]Strain numbers (NRRL) from Agricultural Research Service Culture Collection, Peoria, Illinois, USA.

[c]Indicates mean aflatoxin production (B_1, B_2 and G_1, G_2) in μg/mL and (standard deviation).

[d]Indicates mean *O*-methylsterigmatocystin production (OMST) in μg/mL and (standard deviation).

[e]Indicates mean cyclopiazonic acid (CPA) production in μg/mL and (standard deviation).

[f]Cluster MLST refers to the collapsing of DNA sequences comprising the loci within the aflatoxin cluster (chr. 3).

Table 2 Continued

[g]Genome MLST incorporates all loci examined into the collapsing of DNA sequences.

[h]For each cross, ascospores from different ascocarps were examined separately. Individual progeny ascospores are designated as Parent 1 × Parent 2-ascocarp number-ascospore number.

*Indicates the toxin concentration value is statistically different than the A. flavus parent (IC278) for that particular cross.

**Indicates the toxin concentration value is statistically different than the A. parasiticus parent (IC327, IC65, IC324 or IC33) for that particular cross.

***Indicates the toxin concentration value is statistically different than either parent in that particular cross.

Table 3. Predicted genes on the right arm of chromosome 3 of *Aspergillus flavus*

Protein ID	Genbank Accession	TIGR gene prediction
2911.m00826	EED51201.1	Nonribosomal peptide synthase, putative
2911.m00825	EED51200.1	Hypothetical protein
2911.m00824	EED51199.1	Hypothetical protein
2911.m00823	EED51198.1	Hypothetical protein
2911.m00822	EED51197.1	ABC multidrug transporter, putative
2911.m00821	EED51196.1	Amino acid permease family protein
2911.m00820	EED51195.1	Conserved hypothetical protein
2911.m00819	EED51194.1	Hypothetical protein
2911.m00818	EED51193.1	Hypothetical protein
2911.m00817	EED51192.1	Gluconolactone oxidase, putative
2911.m00816	EED51191.1	Hypothetical protein
2911.m00815	EED51190.1	Fungal specific transcription factor domain containing protein
2911.m00814	EED51189.1	Lignostilbene dioxygenase family protein
2911.m00813	EED51188.1	Hypothetical protein
2911.m00812	EED51187.1	Amidohydrolase family protein
2911.m00811	EED51186.1	Serine protease prots-related
2911.m00810	EED51185.1	Hypothetical protein
2911.m00809	EED51184.1	Fungal specific transcription factor domain containing protein
2911.m00808	EED51183.1	NAD dependent epimerase/dehydratase family protein (*pks/nrps*)
2911.m00807	EED51182.1	Dimethylallyl tryptophan synthase, putative (*dmaT*)
2911.m00806	EED51181.1	Hypothetical protein (*maoA*)
2911.m00805	EED51180.1	Major facilitator superfamily protein (*mfs1*)
2911.m00804	EED51178.1	*aflF* / *norB* / dehydrogenase aflatoxin
2911.m00803[1]	EED51177.1[1]	*aflU*/*cypA*/P450 monooxygenase (43-340)[1]
2911.m00802[1]	EED51177.1[1]	*aflU*/*cypA*/P450 monooxygenase (341-603, 697-1038)[1]

Table 3 Continued

2911.m00801	EED51176.1	*aflT* / *aflT* / transmembrane protein aflatoxin
2911.m00800	EED51175.1	*aflC* / *pksA* / *pksL1* / polyketide synthase aflatoxin
2911.m00799	NA[2, 3]	Hypothetical protein
2911.m00798	EED51174.1	*aflCa* / *hypC* / hypothetical protein aflatoxin
2911.m00797	EED51173.1	*aflD* / *nor-1* / reductase aflatoxin
2911.m00796	EED51172.1	*aflA* / *fas-2* / *hexA* / fatty acid synthase alpha subunit aflatoxin
2911.m00795	EED51171.1	*aflB* / *fas-1* / fatty acid synthase beta subunit aflatoxin
2911.m00794	EED51170.1	*aflR* / *apa-2* / *afl-2* / transcription activator aflatoxin
2911.m00793	EED51169.1	*aflS*/ pathway regulator aflatoxin
2911.m00792	EED51168.1	Aflatoxin biosyntheses short-chain alcohol dehydrogenases AdhA
2911.m00791	EED51167.1	*aflJ*/ *estA*/ esterase aflatoxin
2911.m00790	EED51166.1	*aflE*/ *norA*/ *aad*/ *adh-2*/ NOR reductase/ dehydrogenase aflatoxin
2911.m00789	EED51165.1	*aflM*/ *ver-1*/ dehydrogenase/ ketoreductase aflatoxin
2911.m00788	EED51163.1	*aflN*/ *verA*/ monooxygenase aflatoxin
2911.m00787	EED51162.1	*aflNa*/ *hypD*/ hypothetical protein aflatoxin
2911.m00786	EED51161.1	*aflG*/ *avnA*/ *ord-1*/ cytochrome P450 monooxygenase aflatoxin
2911.m00785	EED51160.1	*aflL*/ *verB*/ desaturase/ P450 monooxygenase aflatoxin
2911.m00784	EED51159.1	*aflLa*/ *hypB*/ hypothetical protein aflatoxin
2911.m00783	EED51158.1	Aflatoxin biosynthesis averufin dehydrogenase *AvfA*
2911.m00782	EED51157.1	*aflO*/ *omtB*/ *dmtA*/ O-methyltransferase B aflatoxin
2911.m00781	EED51156.1	*aflP*/ *omtA*/ *omt-1*/ O-methyltransferase A aflatoxin
2911.m00780	EED51155.1	*aflQ*/ *ordA*/ *ord-1*/ oxidoreductase/ cytochrome P450 monooxigenase aflatoxin
2911.m00779	EED51154.1	*aflK*/ *vbs*/ VERB synthase aflatoxin
2911.m00778	EED51153.1	*aflV*/ *cypX*/ cytochrome P450 monooxygenase aflatoxin
2911.m00777	EED51152.1	*aflW*/ *moxY*/ monooxygenase aflatoxin
2911.m00776	EED51151.1	*aflX*/ *ordB*/ monooxygenase/ oxidase aflatoxin
2911.m00775	EED51150.1	*aflY*/ *hypA*/ *hypP*/ hypothetical protein aflatoxin
2911.m00774	EED51149.1	*aflYa*/ *nadA*/ NADH oxidase aflatoxin

Table 3 Continued

2911.m00773	NA[3, 4]	NADH oxidase, putative (*hxtA*)
2911.m00772	EED51148.1	Hexose transporter, putative (*glcA*)
2911.m00771	EED51147.1	Alpha-glucosidase/alpha-amylase, putative (*sugR*)
2911.m00770	EED51146.1	Transcriptional regulator, putative
2911.m00769	EED51145.1	Ser/Thr protein phosphatase family protein
2911.m00768	EED51144.1	Major facilitator superfamily protein
2911.m00767	EED51143.1	ATPase, AAA family protein
2911.m00766	EED51142.1	Hypothetical protein
2911.m00765	EED51141.1	ATPase, AAA family protein
2911.m00764	EED51140.1	Hypothetical protein
2911.m00763	EED51139.1	Hypothetical protein
2911.m00762	EED51138.1	Major facilitator superfamily protein
2911.m00761	EED51137.1	Hypothetical protein
2911.m00760	EED51136.1	Sterol 4-a-methyl-oxidase-related
2911.m00759	EED51135.1	Hypothetical protein
2911.m00758	EED51134.1	Hypothetical protein
2911.m00757	EED51133.1	Oxidoreductase, FAD/FMN-binding family protein
2911.m00756	EED51132.1	Hypothetical protein
2911.m00755	EED51131.1	Oxidoreductase, short chain dehydrogenase/reductase family protein
2911.m00754	EED51130.1	Oxidoreductase, zinc-binding dehydrogenase family protein
2911.m00753	EED51129.1	Flavin-binding monooxygenase-like family protein
2911.m00752	EED51128.1	Fungal-specific transcription factor domain containing protein
2911.m00751	EED51127.1	Flavin-binding monooxygenase-like family protein
2911.m00750	EED51126.1	Metallo-beta-lactamase superfamily protein
2911.m00749	EED51125.1	Major facilitator superfamily protein
2911.m00748	EED51124.1	Hypothetical protein
2911.m00747	EED51123.1	Protein kinase domain containing protein
2911.m00746	EED51122.1	Conserved hypothetical protein

Table 3 Continued

2911.m00745	EED51121.1	Glycosyl hydrolases family 16 protein

[1]The gene models for 2911.m00802 and 2911.m00803 were merged together under the same EED51177.1 Genbank accession. The corresponding spans within the TIGR gene prediction (*aflU*/*cypA*/P450 monooxygenase) are indicated within parentheses.

[2]The gene model for 2911.m00779 was deleted because it was merged with the neighboring 2911.m00800 (*aflC* / *pksA* / *pksL1* / polyketide synthase aflatoxin).

[3]NA = not available.

[4]The gene model for 2911.m00773 was deleted because it was merged with the neighboring 2911.m00774 (*aflYa*/ *nadA*/ NADH oxidase aflatoxin).

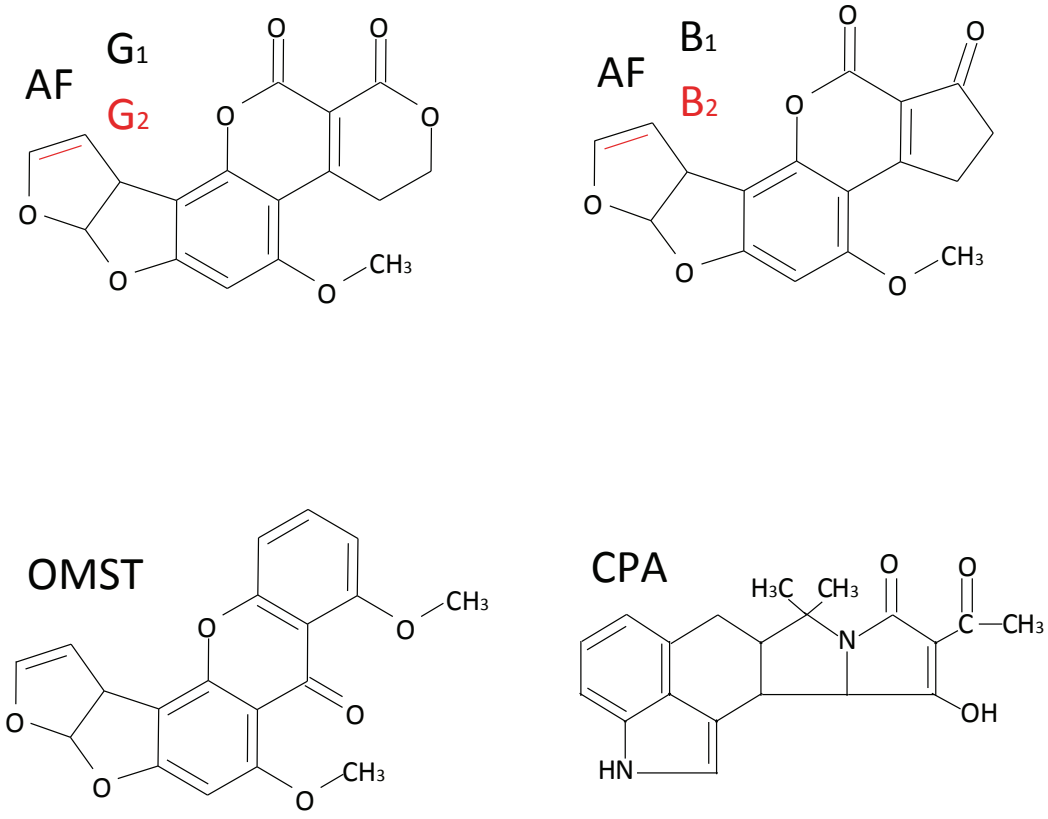

Figure 1. Chemical structures of OMST, B and G aflatoxins, and CPA. Red line segments in the AF G and B molecules denote the double bond distinguishing AF G_2 and B_2 from AF G_1 and B_1, respectively.

Figure 2. Sexual reproductive structures observed in hybrid crosses between *Aspergillus flavus* and *A. parasiticus*. A: Sectioned stroma containing one ascospore-bearing ascocarp; B: SEM image of aborted ascocarp; C: Germinated ascospore, arrow indicates oil droplet inside ascospore; D: SEM image of cross-sectioned stroma with one ascospore-bearing ascocarp, arrow shows ascocarp peridium; E: SEM image showing structure of ascocarp peridium; F: SEM image of ascocarp-bearing ascospore, arrow shows ascocarp peridium; G: Two viable-appearing ascospores containing oil, surrounded by collapsed empty ascospores; H: Ascus containing nine ascospores; I: SEM image showing ascospore with finely tuberculate texture and equatorial ridge; J: SEM image showing detail of ascospore equatorial ridge. Abbreviations: a, ascocarp; h, hypha; m, stromal matrix; p, ascocarp peridium; s, ascospore. Scale bars: 1, 4: 100µm; 2, 3, 5, 6, 7, 8: 10µm; 9, 10: 1µm.

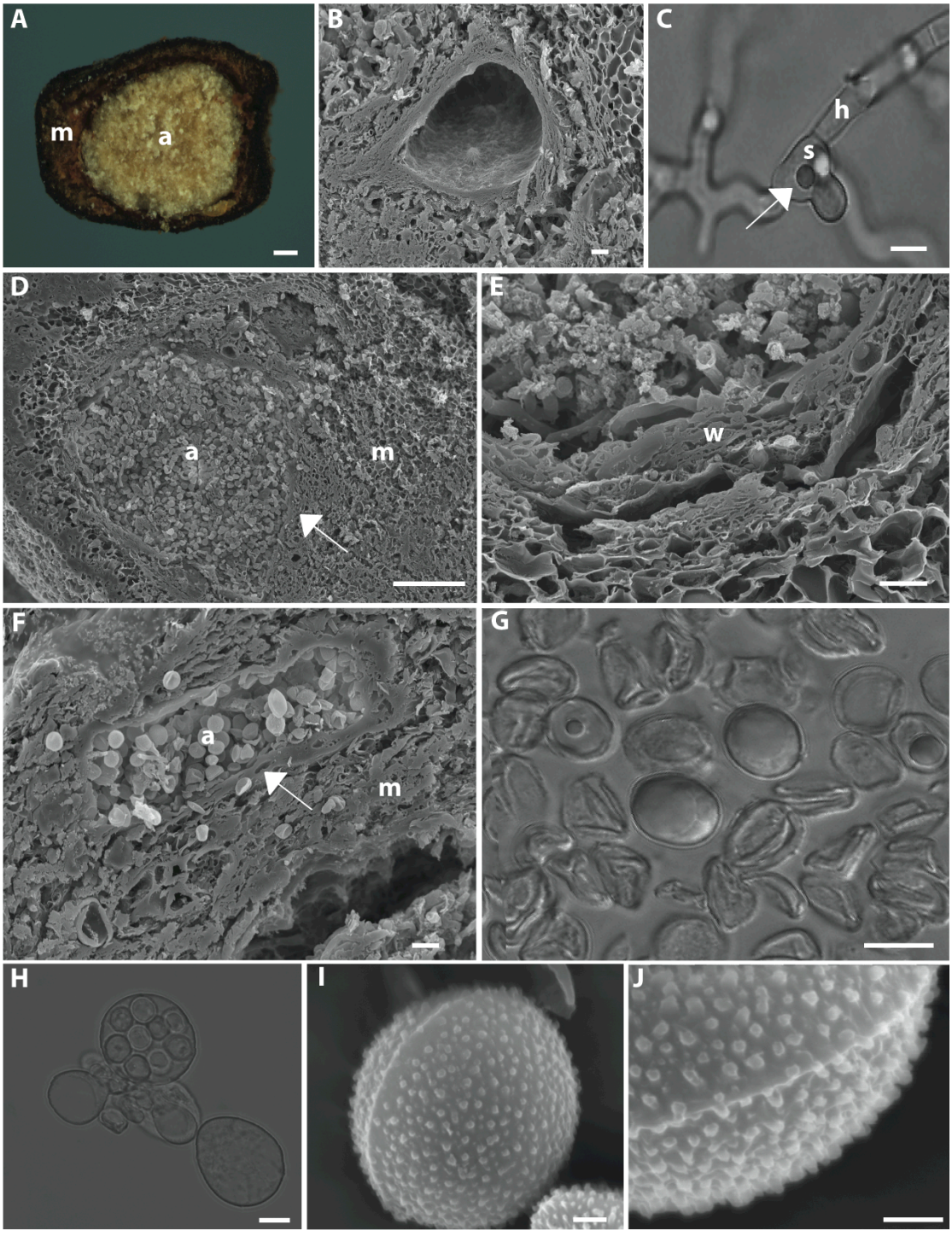
A
m
a
B
C
h
s
D
a
m
E
w
F
a
m
G
H
I
J

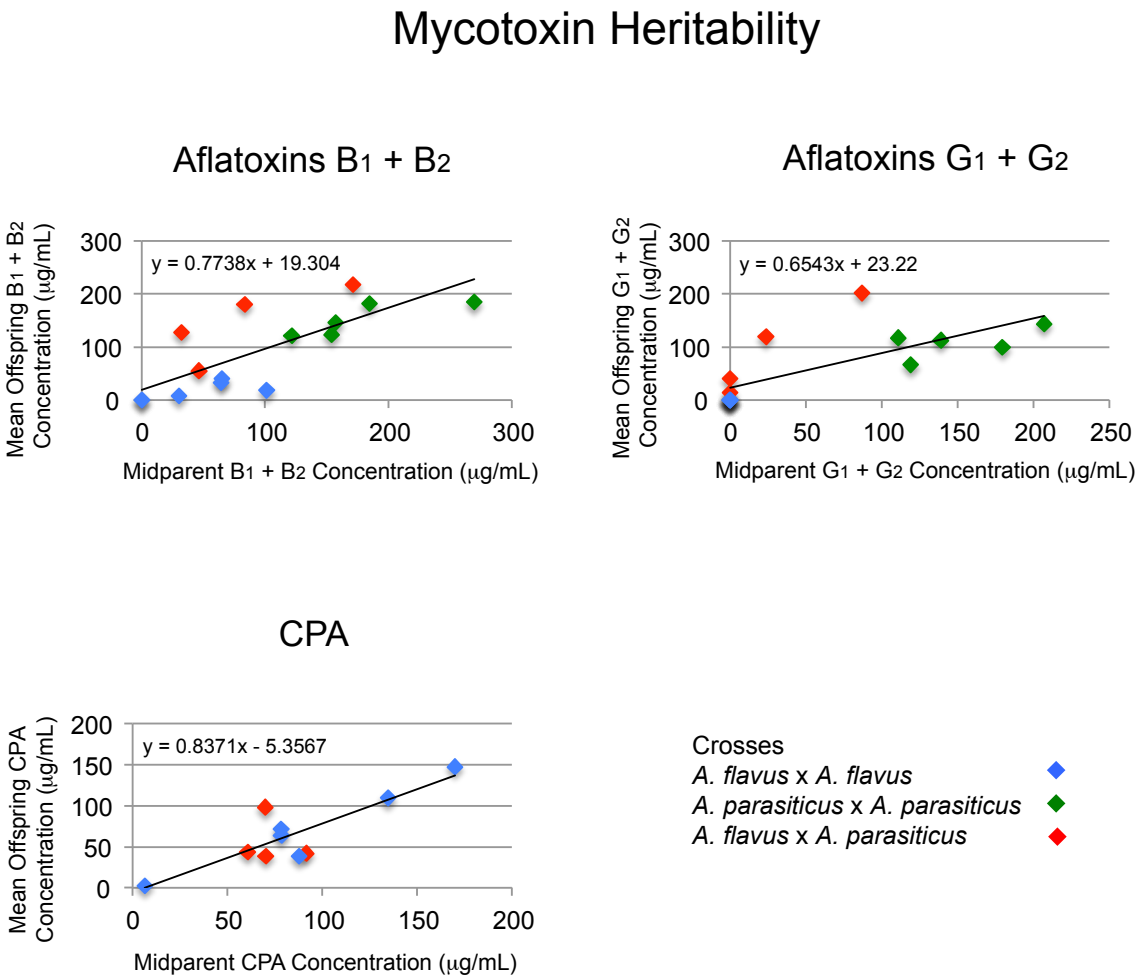

Figure 3. Aflatoxin and CPA heritability in intra and interspecific crosses of *A. flavus* and *A. parasiticus*. Each blue diamond denotes the value of the mean offspring toxin concentration versus midparent toxin concentration for each *A. flavus* x *A. flavus* cross; each green diamond denotes the value of mean offspring toxin concentration versus midparent toxin concentration for each *A. parasiticus* x *A. parasiticus* cross; and each red diamond denotes the value of mean offspring toxin concentration versus midparent toxin concentration for each hybrid *A. flavus* x *A. parasiticus* cross.

Figure 4. Genome-wide similarity dendrogram based on aCGH data of a representative sample of fifty-six isolates representing variation in intra and interspecific crosses, natural isolates sampled from populations of *A. flavus* and *A. parasiticus* and closely related species in *Aspergillus* section *Flavi.* Red squares indicate the highest level of similarity among the individuals in a particular grouping, while blue indicates the lowest level of similarity. Hybrid progeny individuals and clades are denoted with red lettering and lines, respectively. Individuals are grouped according to similarity with respect to the reference strain.

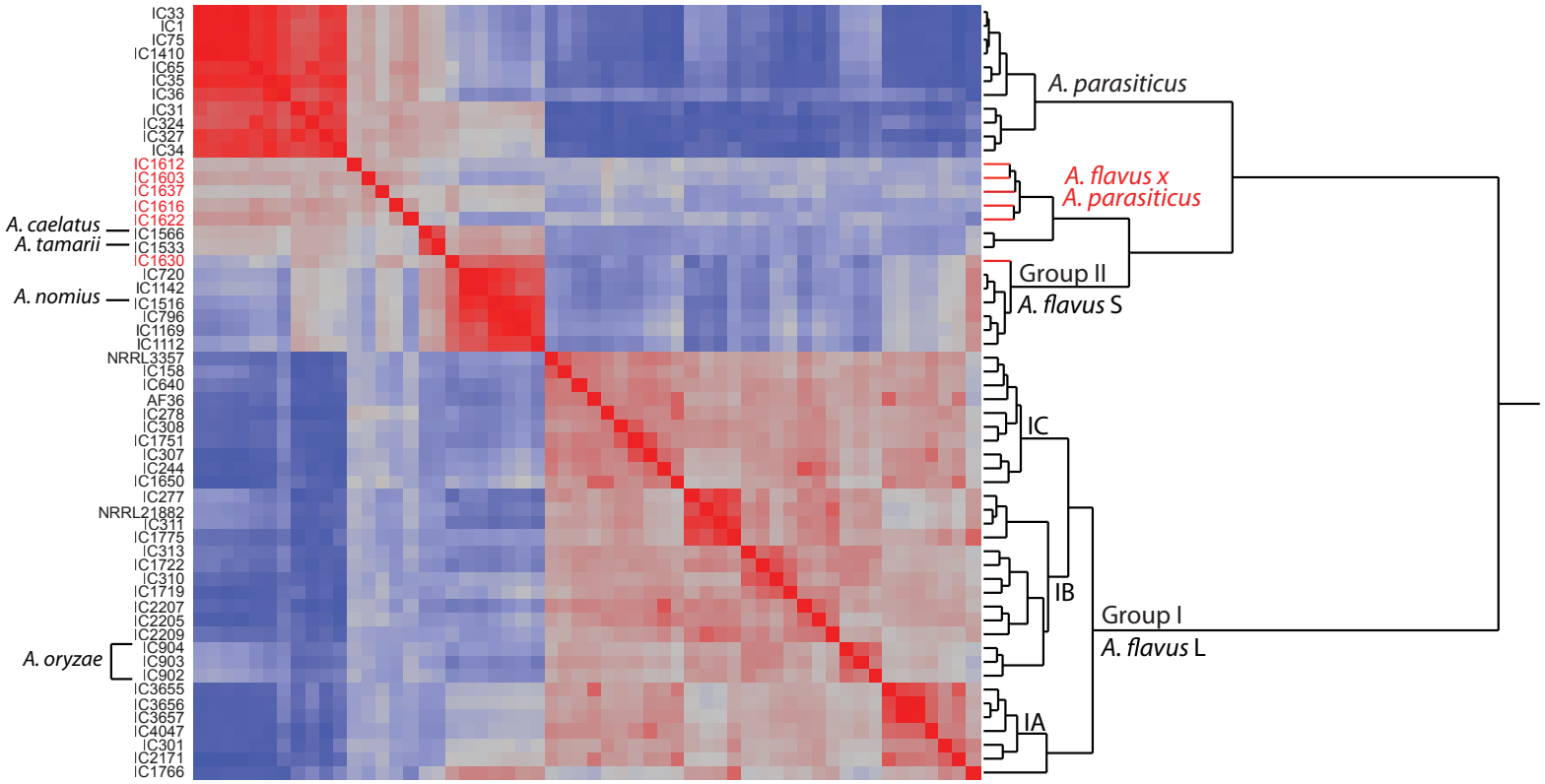
IC33
IC1
IC75
IC1410
IC65
IC35
IC36
IC31
IC324
IC327
IC34
IC1612
IC1603
IC1637
IC1616
IC1622
IC1566
IC1533
IC1630
IC720
IC1142
IC1516
IC796
IC1169
IC1112
NRRL3357
IC158
IC640
AF36
IC278
IC308
IC1751
IC307
IC244
IC1650
IC277
NRRL21882
IC311
IC1775
IC313
IC1722
IC310
IC1719
IC2207
IC2205
IC2209
IC904
IC903
IC902
IC3655
IC3656
IC3657
IC4047
IC301
IC2171
IC1766
A. caelatus
A. tamarii
A. nomius
A. oryzae
A. parasiticus
A. flavus x
A. parasiticus
Group II
A. flavus S
IC
IB
IA
Group I
A. flavus L

Figure 5. Heat maps showing aCGH patterns in the CPA, aflatoxin and sugar clusters in the right arm of chromosome 3; the strains are ordered based on clades inferred from genome-wide aCGH analysis in Figure 4. Red bars indicate the highest level of hybridization of the isolate to the reference strain at a particular gene region. Blue bars indicate the lowest level of hybridization to the reference strain. Yellow, green and aqua indicate some median level of hybridization. Individuals are grouped according to dendrogram in Figure 4

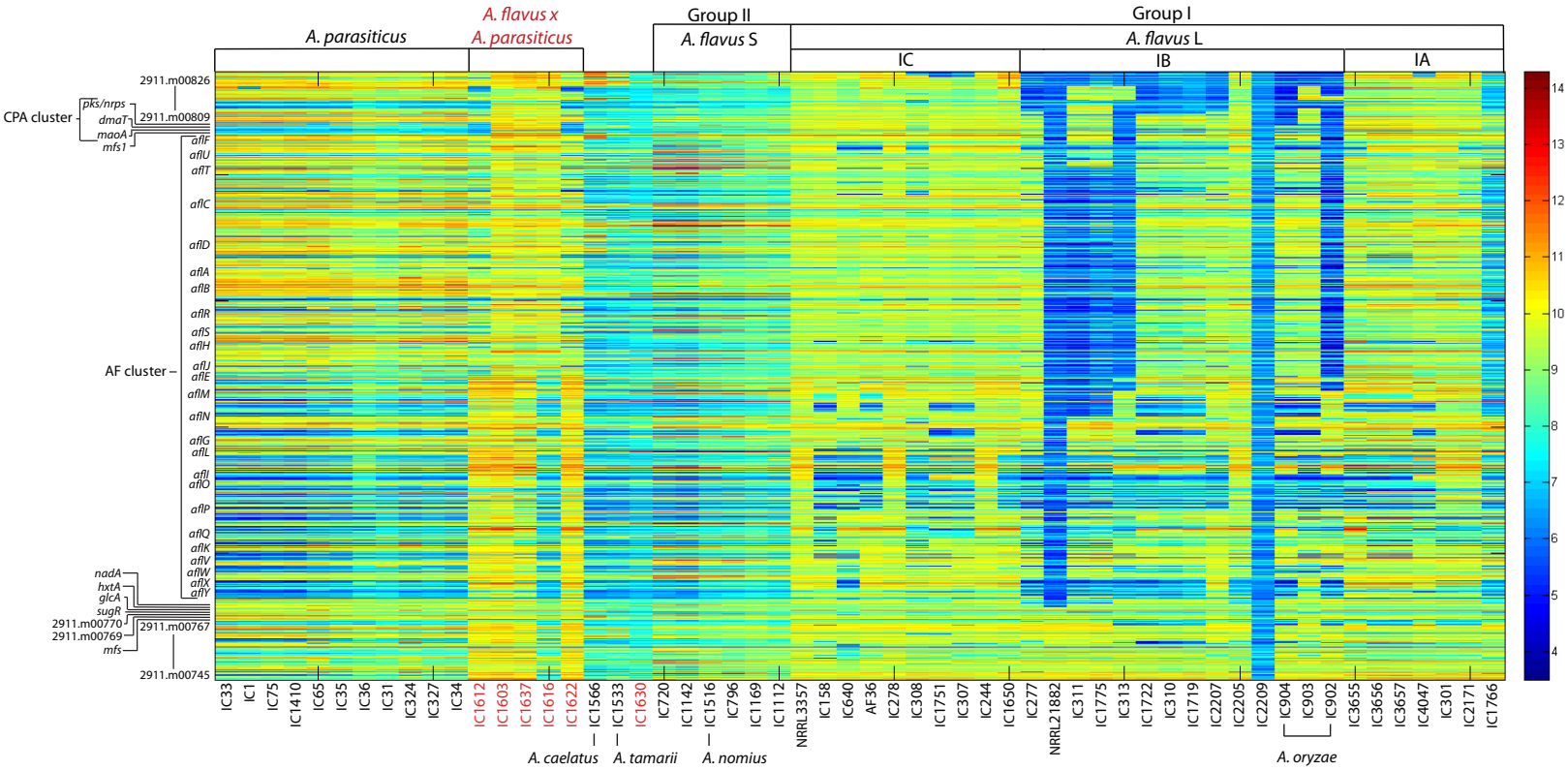
A. parasiticus
A. flavus x A. parasiticus
Group II
A. flavus S
Group I
A. flavus L
IC
IB
IA
CPA cluster
AF cluster
2911.m00826
pks/nrps
2911.m00809
dmaT
maoA
mfs1
aflF
aflU
aflT
aflC
aflD
aflA
aflB
aflR
aflS
aflH
aflJ
aflE
aflM
aflN
aflG
aflL
aflJ
aflO
aflP
aflQ
aflK
aflV
aflW
aflX
aflY
nadA
hxtA
glcA
sugR
2911.m00770
2911.m00769
mfs
2911.m00767
2911.m00745
IC33
IC1
IC75
IC1410
IC65
IC35
IC36
IC31
IC324
IC327
IC34
IC1612
IC1603
IC1637
IC1616
IC1622
IC1566
IC1533
IC1630
IC720
IC1142
IC1516
IC796
IC1169
IC1112
NRRL3357
IC158
IC640
AF36
IC278
IC308
IC1751
IC307
IC244
IC1650
IC277
NRRL21882
IC311
IC1775
IC313
IC1722
IC310
IC1719
IC2207
IC2205
IC2209
IC904
IC903
IC902
IC3655
IC3656
IC3657
IC4047
IC301
IC2171
IC1766
A. caelatus
A. tamarii
A. nomius
A. oryzae
14
13
12
11
10
9
8
7
6
5
4

Figure 6. Heat maps of six *Aspergillus flavus* and *A. parasiticus* parent-offspring trios for the chromosomal region shown in Figure 5. In each trio plot, the center plot is the progeny individual, flanked on the left side by the *A. flavus* parent and flanked on the right side by the *A. parasiticus* parent. Red bars indicate the highest level of hybridization of the isolate to the reference strain at a particular gene region. Blue bars indicate the lowest level of hybridization to the reference strain. Yellow, green and aqua indicate some median level of hybridization. The blue line between plots is an indication of greater similarity to either the *A. flavus* parent (approaching 1.0) or greater similarity to the *A. parasiticus* parent (approaching 0.0.) Black horizontal bars indicate putative crossover recombination breakpoints where progeny hybridization patterns transition from one parent to the other.

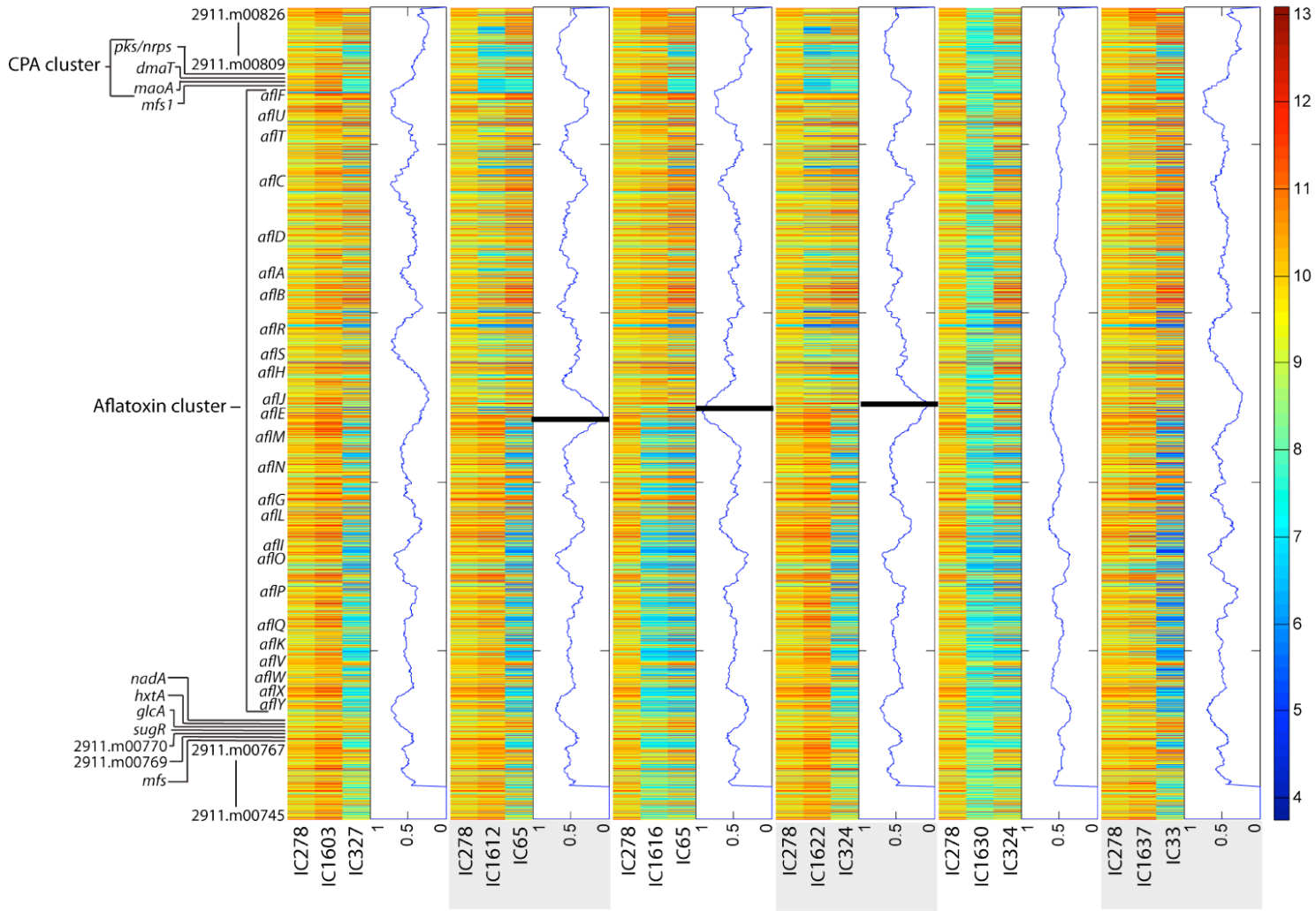
2911.m00826
CPA cluster
pks/nrps
dmaT
2911.m00809
maoA
mfs1
aflF
aflU
aflT
aflC
aflD
aflA
aflB
aflR
aflS
aflH
aflJ
aflE
Aflatoxin cluster
aflM
aflN
aflG
aflL
aflI
aflO
aflP
aflQ
aflK
aflV
aflW
aflX
aflY
nadA
hxtA
glcA
sugR
2911.m00770
2911.m00769
mfs
2911.m00767
2911.m00745
IC278
IC1603
IC327
IC278
IC1612
IC65
IC278
IC1616
IC65
IC278
IC1622
IC324
IC278
IC1630
IC324
IC278
IC1637
IC33
1
0.5
0
13
12
11
10
9
8
7
6
5
4

A

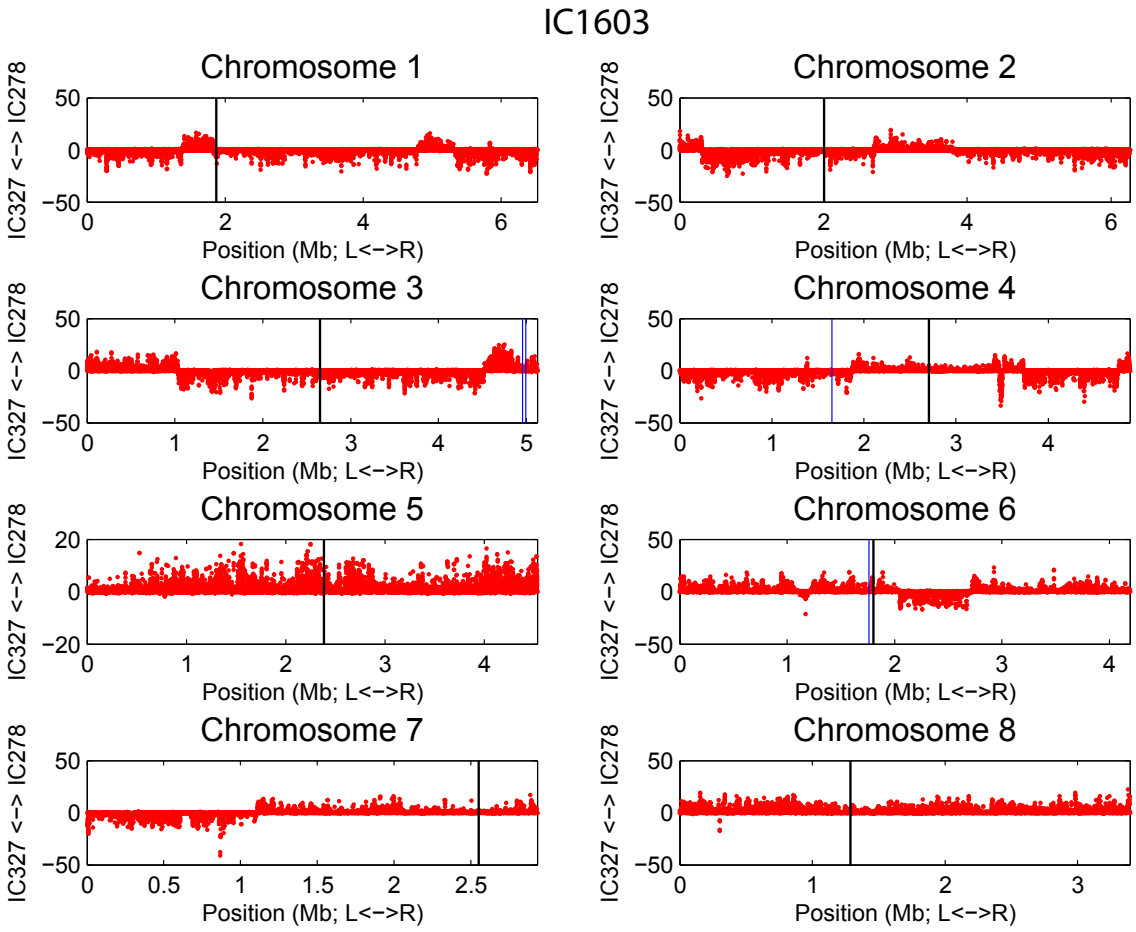

Figure 7a. Genome-wide parentage plot for hybrid progeny isolate IC1603. Each red point represents a probe on the array. As dots approach the positive value on the y-axis, this indicates a hybridization pattern more similar to the *A. flavus* parent; as dots approach the negative value, this indicates a hybridization pattern more similar to the *A. parasiticus* parent. Black vertical lines represent the putative centromere location on each chromosome. Blues lines represent MLST loci: *aflM* and *aflW* on chromosome 3, *trpC* on chromosome 4 and *MAT* on chromosome 6.

B

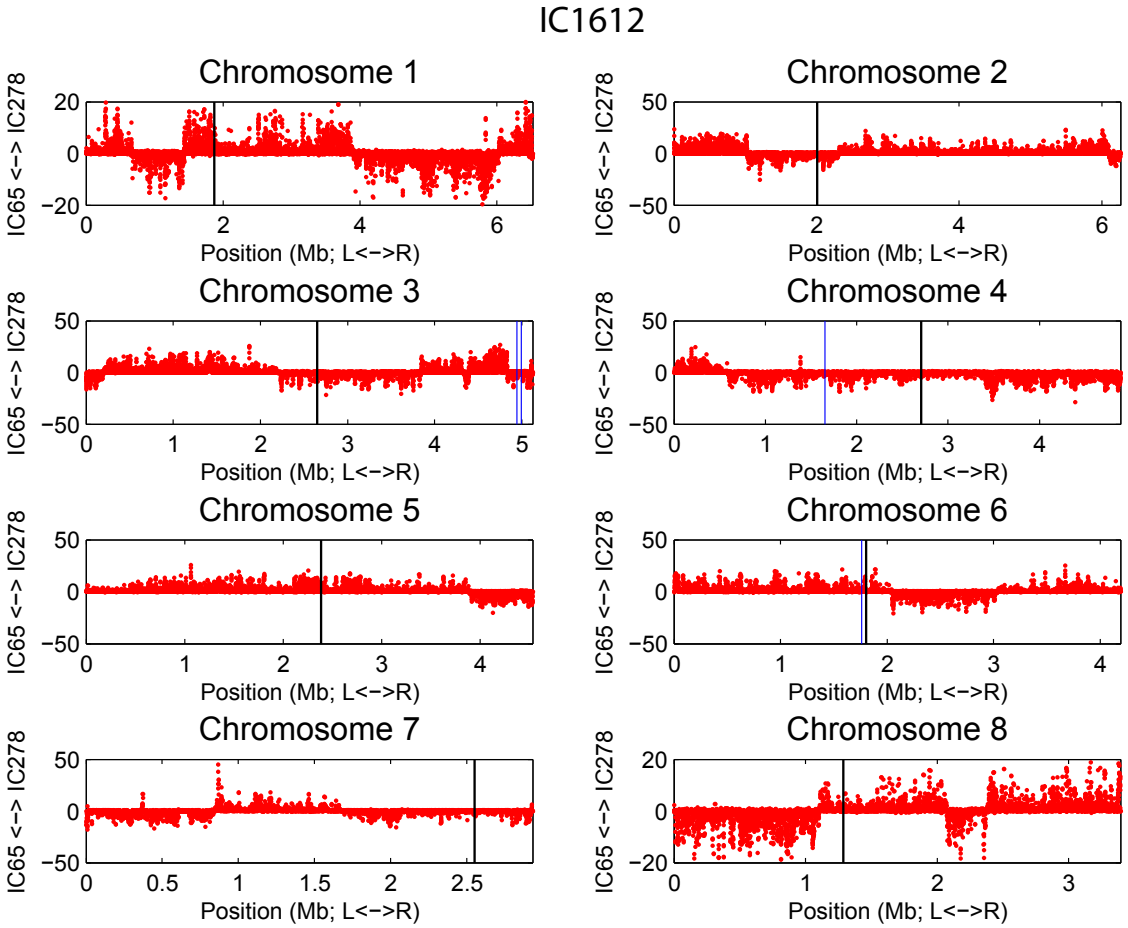

Figure 7b. Genome-wide parentage plot for hybrid progeny isolate IC1612. Each red point represents a probe on the array. As dots approach the positive value on the y-axis, this indicates a hybridization pattern more similar to the *A. flavus* parent; as dots approach the negative value, this indicates a hybridization pattern more similar to the *A. parasiticus* parent. Black vertical lines represent the putative centromere location on each chromosome. Blues lines represent MLST loci: *aflM* and *aflW* on chromosome 3, *trpC* on chromosome 4 and *MAT* on chromosome 6.

C

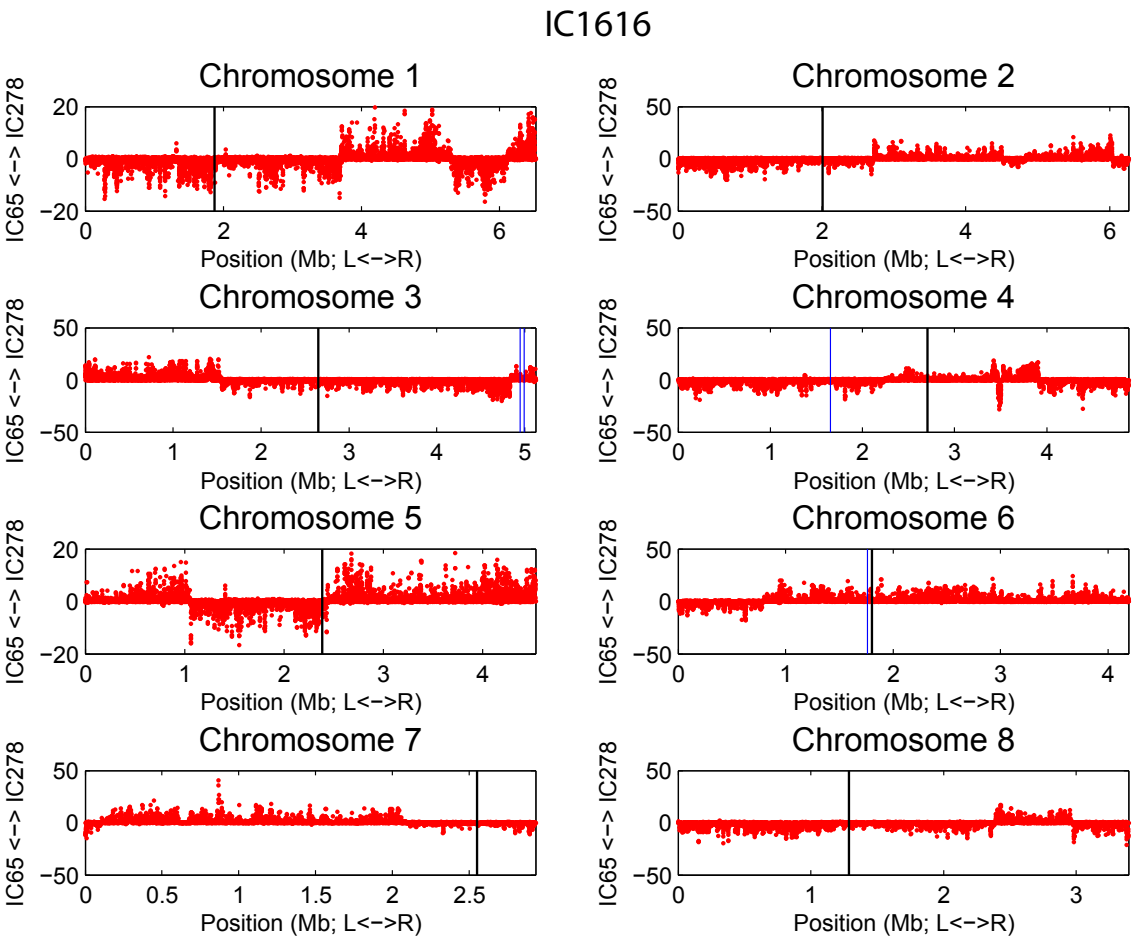

Figure 7c. Genome-wide parentage plot for hybrid progeny isolate IC1616. Each red point represents a probe on the array. As dots approach the positive value on the y-axis, this indicates a hybridization pattern more similar to the *A. flavus* parent; as dots approach the negative value, this indicates a hybridization pattern more similar to the *A. parasiticus* parent. Black vertical lines represent the putative centromere location on each chromosome. Blues lines represent MLST loci: *aflM* and *aflW* on chromosome 3, *trpC* on chromosome 4 and *MAT* on chromosome 6.

D

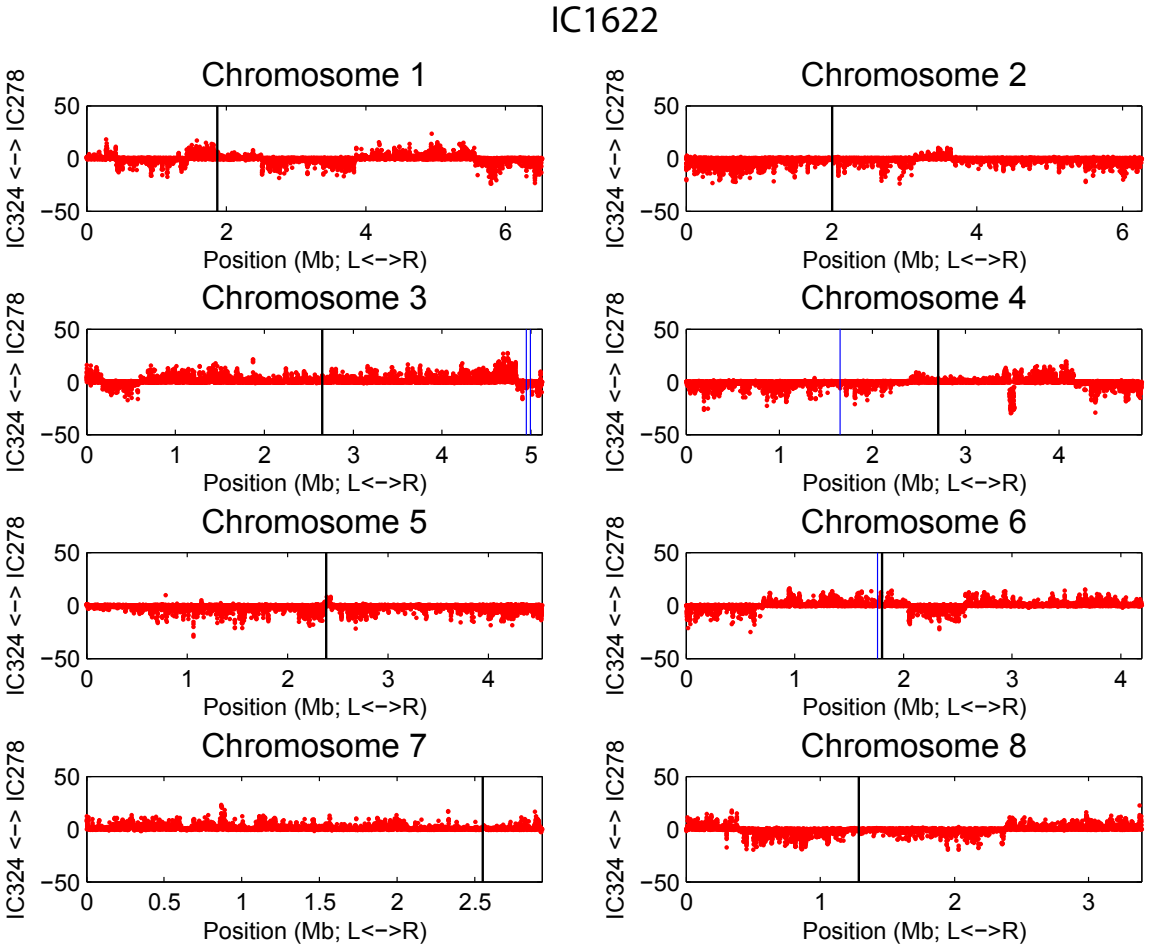

Figure 7d. Genome-wide parentage plot for hybrid progeny isolate IC1622. Each red point represents a probe on the array. As dots approach the positive value on the y-axis, this indicates a hybridization pattern more similar to the *A. flavus* parent; as dots approach the negative value, this indicates a hybridization pattern more similar to the *A. parasiticus* parent. Black vertical lines represent the putative centromere location on each chromosome. Blues lines represent MLST loci: *aflM* and *aflW* on chromosome 3, *trpC* on chromosome 4 and *MAT* on chromosome 6.

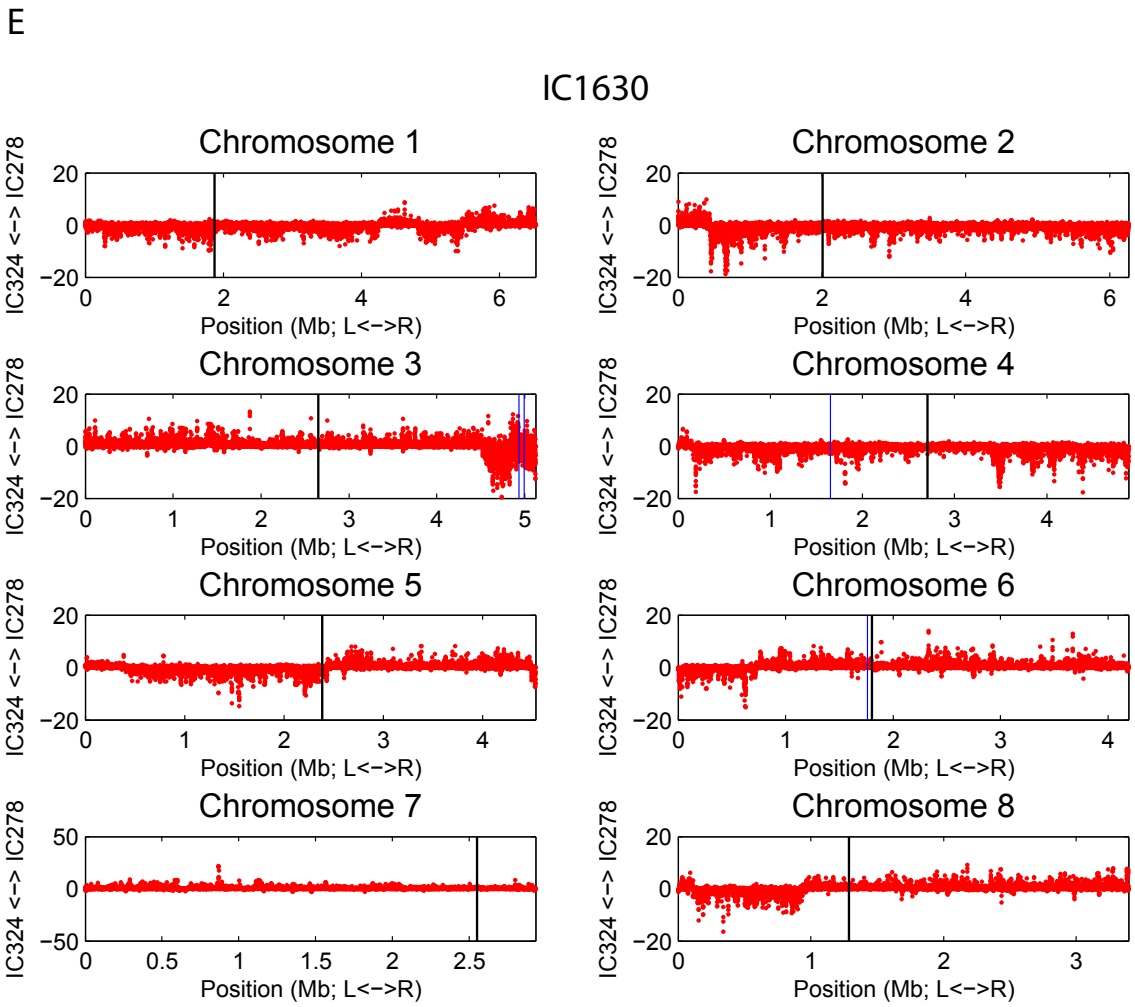

Figure 7e. Genome-wide parentage plot for hybrid progeny isolate IC1630. Each red point represents a probe on the array. As dots approach the positive value on the y-axis, this indicates a hybridization pattern more similar to the *A. flavus* parent; as dots approach the negative value, this indicates a hybridization pattern more similar to the *A. parasiticus* parent. Black vertical lines represent the putative centromere location on each chromosome. Blues lines represent MLST loci: *aflM* and *aflW* on chromosome 3, *trpC* on chromosome 4 and *MAT* on chromosome 6.

F

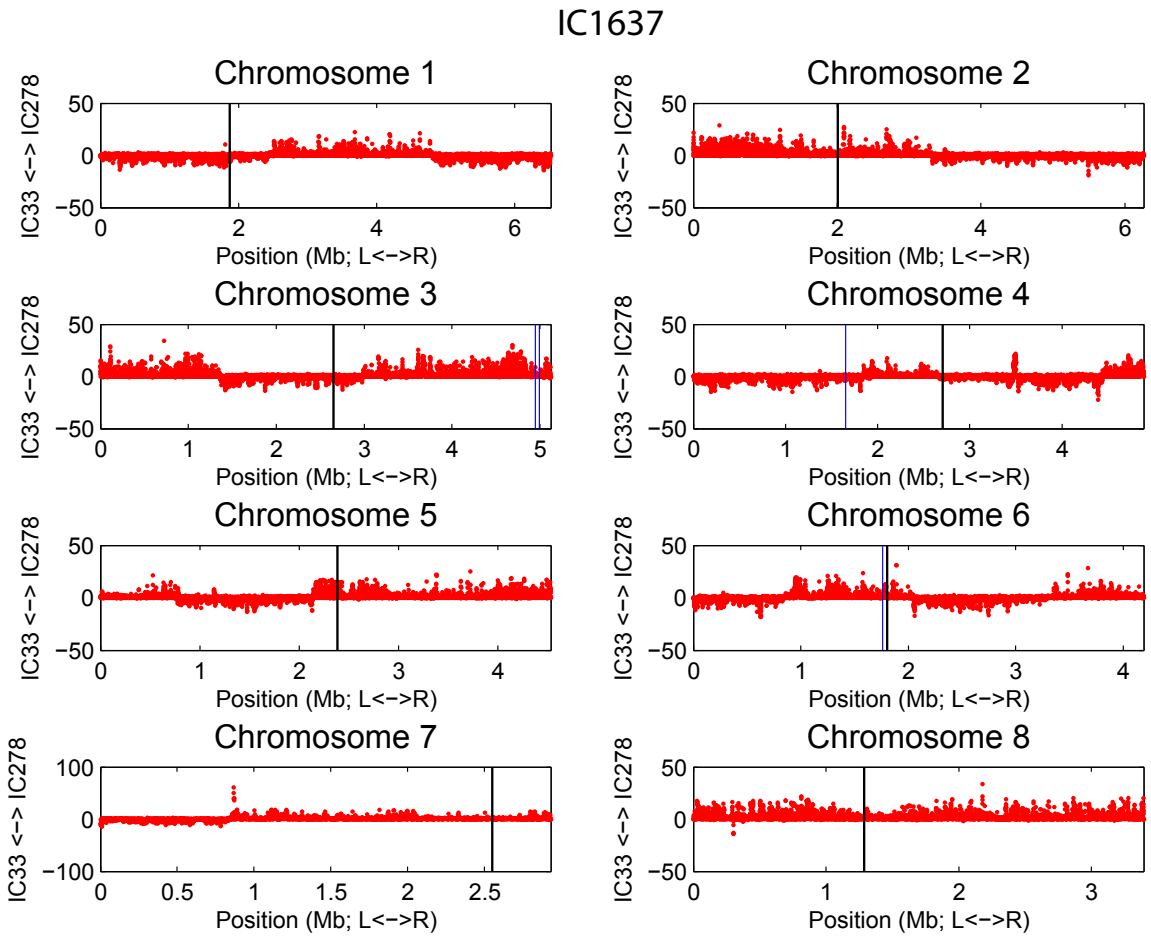

Figure 7f. Genome-wide parentage plot for hybrid progeny isolate IC1637. Each red point represents a probe on the array. As dots approach the positive value on the y-axis, this indicates a hybridization pattern more similar to the *A. flavus* parent; as dots approach the negative value, this indicates a hybridization pattern more similar to the *A. parasiticus* parent. Black vertical lines represent the putative centromere location on each chromosome. Blues lines represent MLST loci: *aflM* and *aflW* on chromosome 3, *trpC* on chromosome 4 and *MAT* on chromosome 6.

Figure 8a. Maximum likelihood phylogenetic and principle component analyses based on MLSTs (*aflM, aflW* and *trpC*) showing clustering and association with quantitative variation in aflatoxin production between experimental hybrid strains and natural isolates of *A. parasiticus*, *A. flavus* L, S_{BG} and S_B sampled from populations on a global scale. Symbols in the PCA plots denote the species; colors in the upper plot indicate geographical location, while colors in the lower plot indicate total aflatoxin concentration values.

A Global Phylogeny and PCA

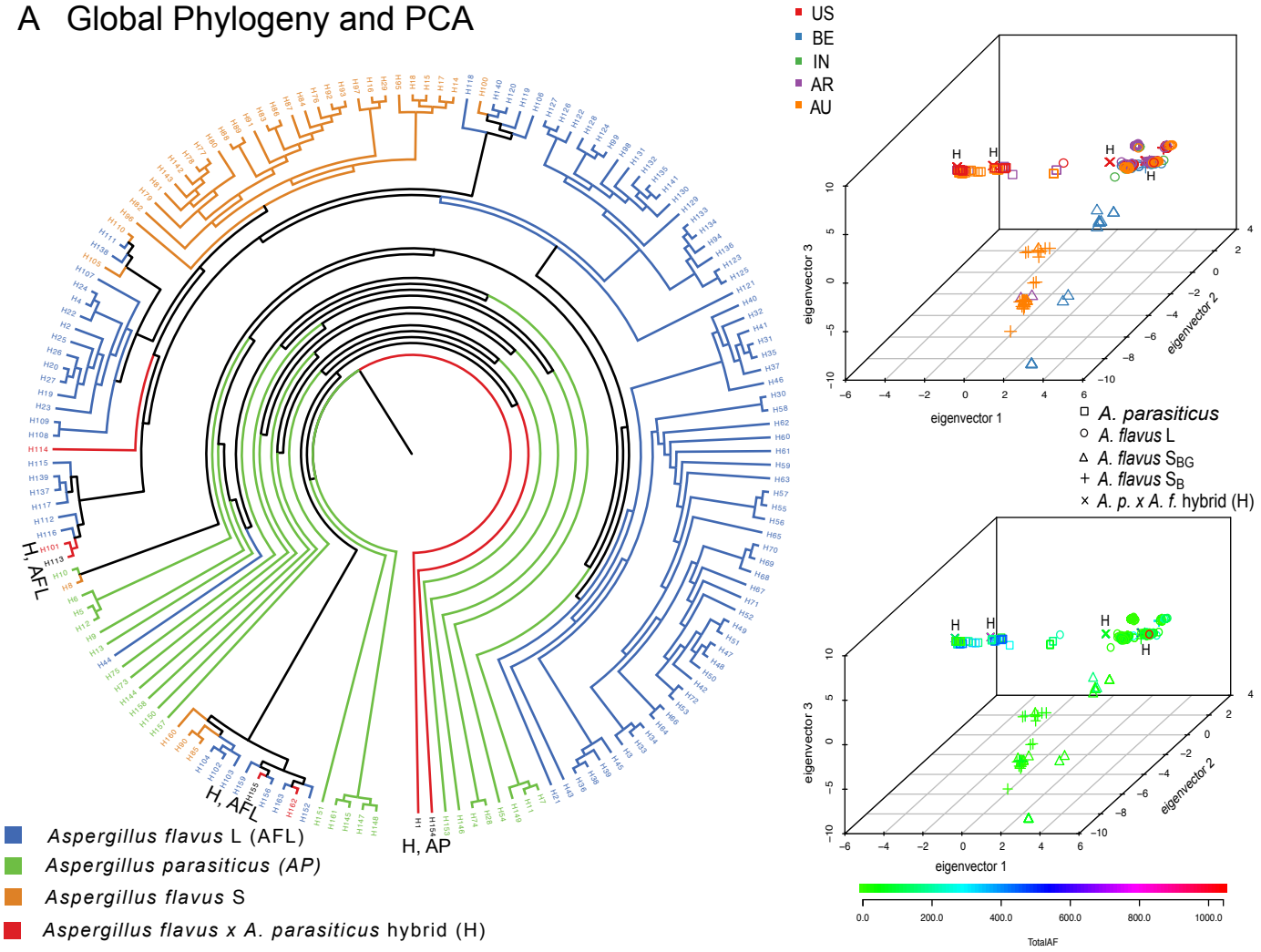

Figure 8b. Maximum likelihood phylogenetic and principle component analyses based on MLSTs (*aflM, aflW* and *trpC*) showing clustering and association with quantitative variation in aflatoxin production between experimental hybrid strains and natural isolates of *A. parasiticus*, *A. flavus* L, S_{BG} and S_B sampled from populations within the US alone. Symbols in the PCA plots denote the species; colors in the upper plot indicate geographical location, while colors in the lower plot indicate total aflatoxin concentration values.
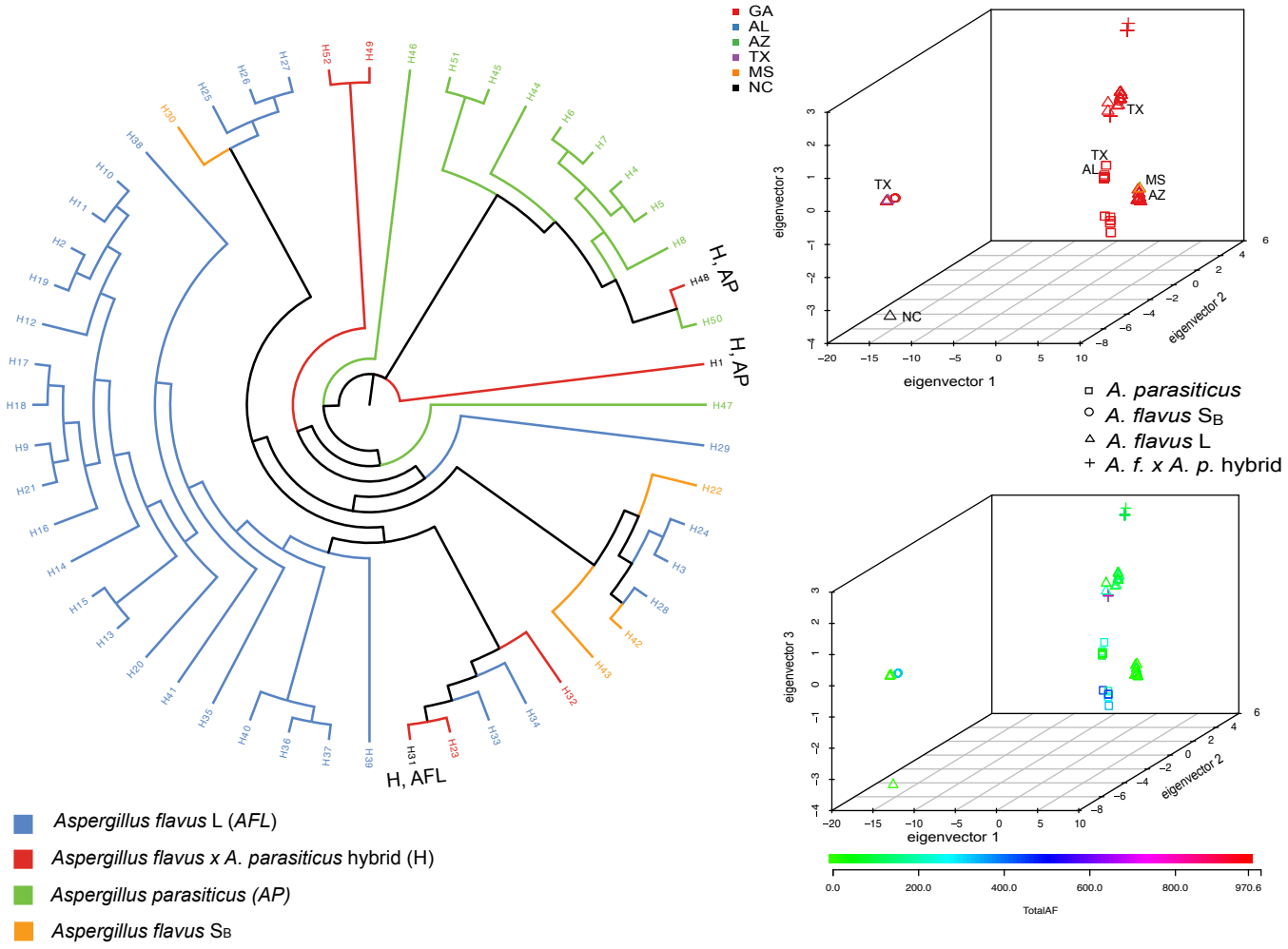
B US Only Phylogeny and PCA